MULTIPLE SCATTERING THEORY OF X-RAY PHOTOELECTRON DIFFRACTION AND ABSORPTION SPECTROSCOPY AS A STRUCTURAL TOOL

Calogero R. Natoli

LNF-INFN, Frascati (Rome), Italy

XAFS JOURNAL CLUB EUROPE AND ASIA - ROME: 06 JULY 2021

MAIN SPECTROSCOPIC TOOLS

- Photo-emission (PE)
- Photo-electron diffraction (PhD)
- Absorption (XAS)
- Resonant elastic x-ray scattering (REXS)
- Low-Energy Electron Diffraction (LEED)
- Electron Energy Loss Spectroscopy (EELS)

PROVIDE STRUCTURAL AND ELECTRONIC INFORMATION IN CONDENSED MATTER PHYSICS

D. Sebilleau et al, J. Phys.: Condens. Matter 18, R175 – R230 (2006)

Photo-emission and Photo-electron diffraction

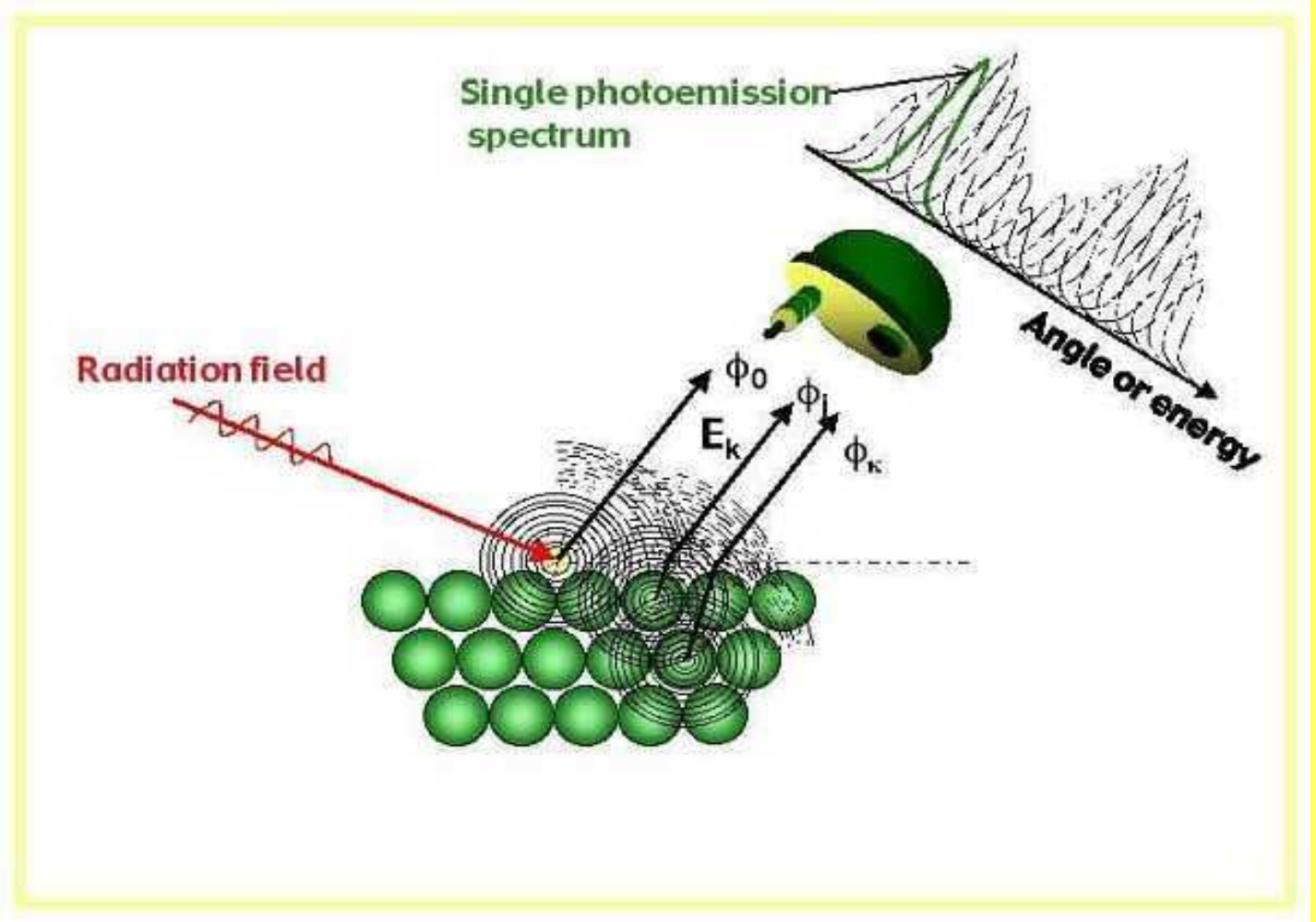

Kas et al Phys. Rev. B 91, 121112(R) (2015)

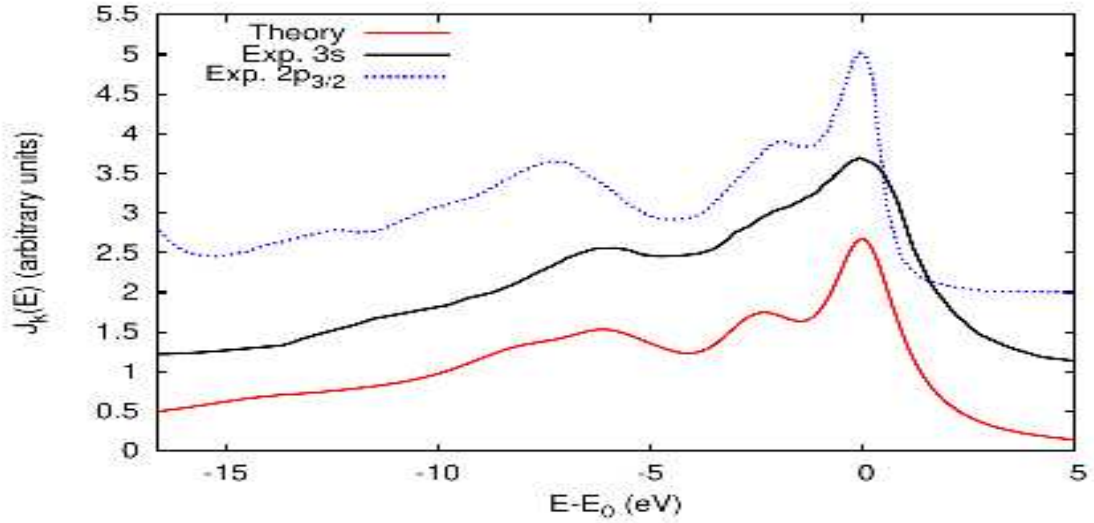

FIG. 3: (color online) Calculated Ni 3s core-level spectrum for NiO (red) compared to experimental 3s (black) $2p_{3/2}$ (blue dashed) XPS results [31].

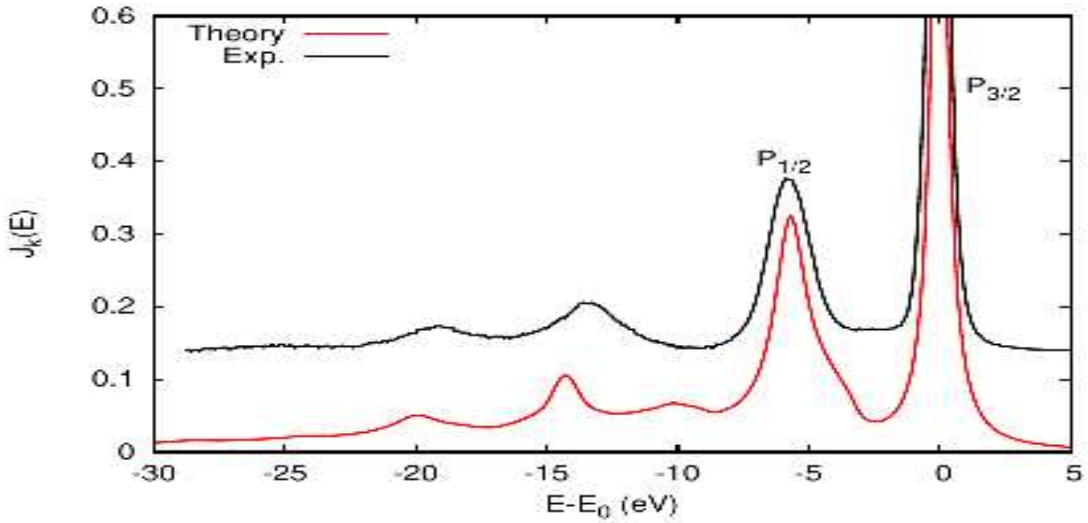

FIG. 1: (color online). Comparison of the calculated XPS using the approach of this work (red) and experimental (black) Ti $2p_{3/2}$ and $2p_{1/2}$ XPS of TiO_2-rutile. Each of the spin-orbit split quasiparticle peaks at 0 and -6 eV, exhibits a strong charge-transfer satellite at an excitation energy $\omega_c \approx 14$ eV below.

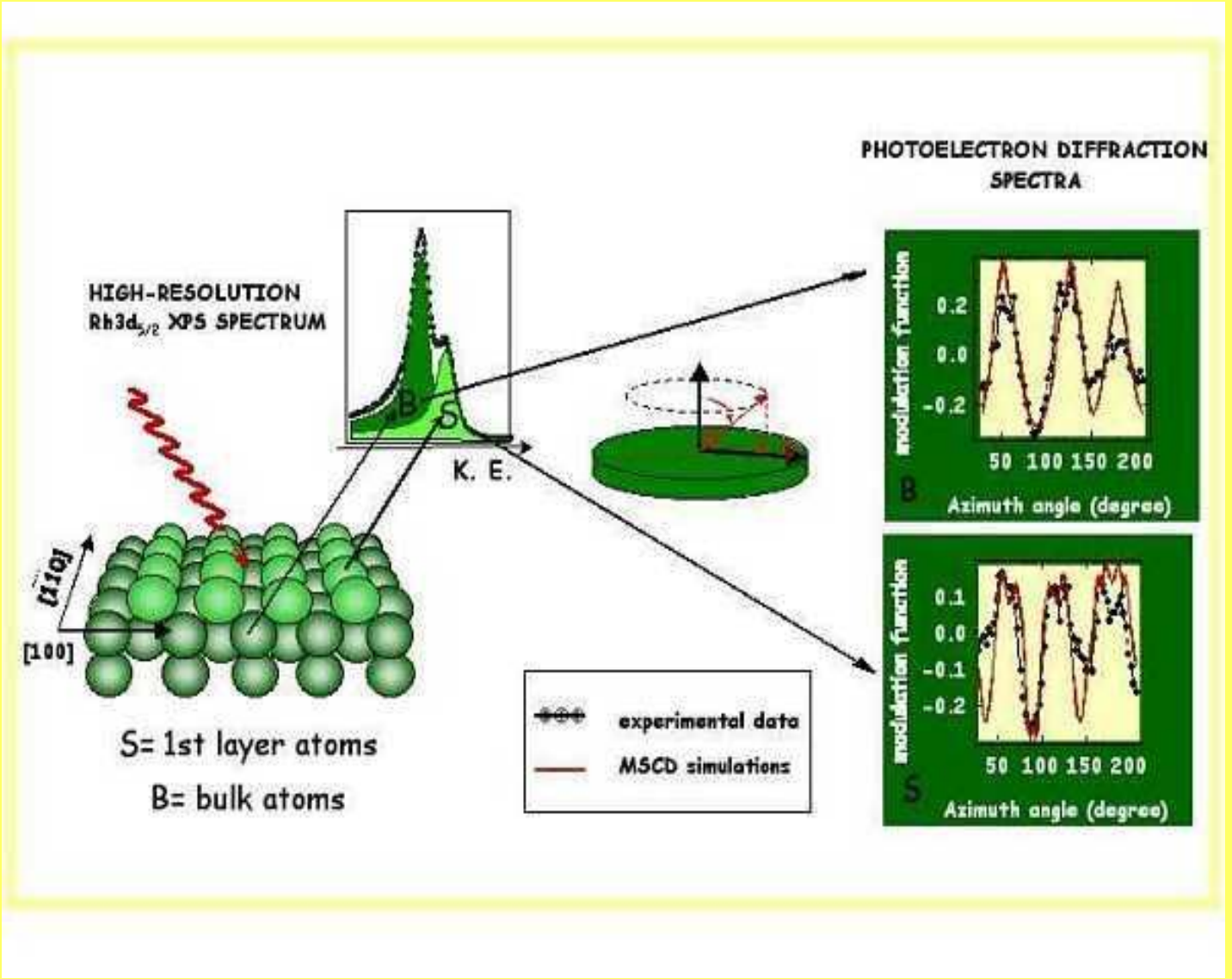
PHOTOELECTRON DIFFRACTION SPECTRA
HIGH-RESOLUTION
Rh3d5/2 XPS SPECTRUM
B
S
K. E.
[1$\bar{1}$0]
[100]
S= 1st layer atoms
B= bulk atoms
experimental data
MSCD simulations
modulation function
0.2
0.0
-0.2
50 100 150 200
B
Azimuth angle (degree)
modulation function
0.1
0.0
-0.1
-0.2
50 100 150 200
S
Azimuth angle (degree)

Photo-electron Diffraction

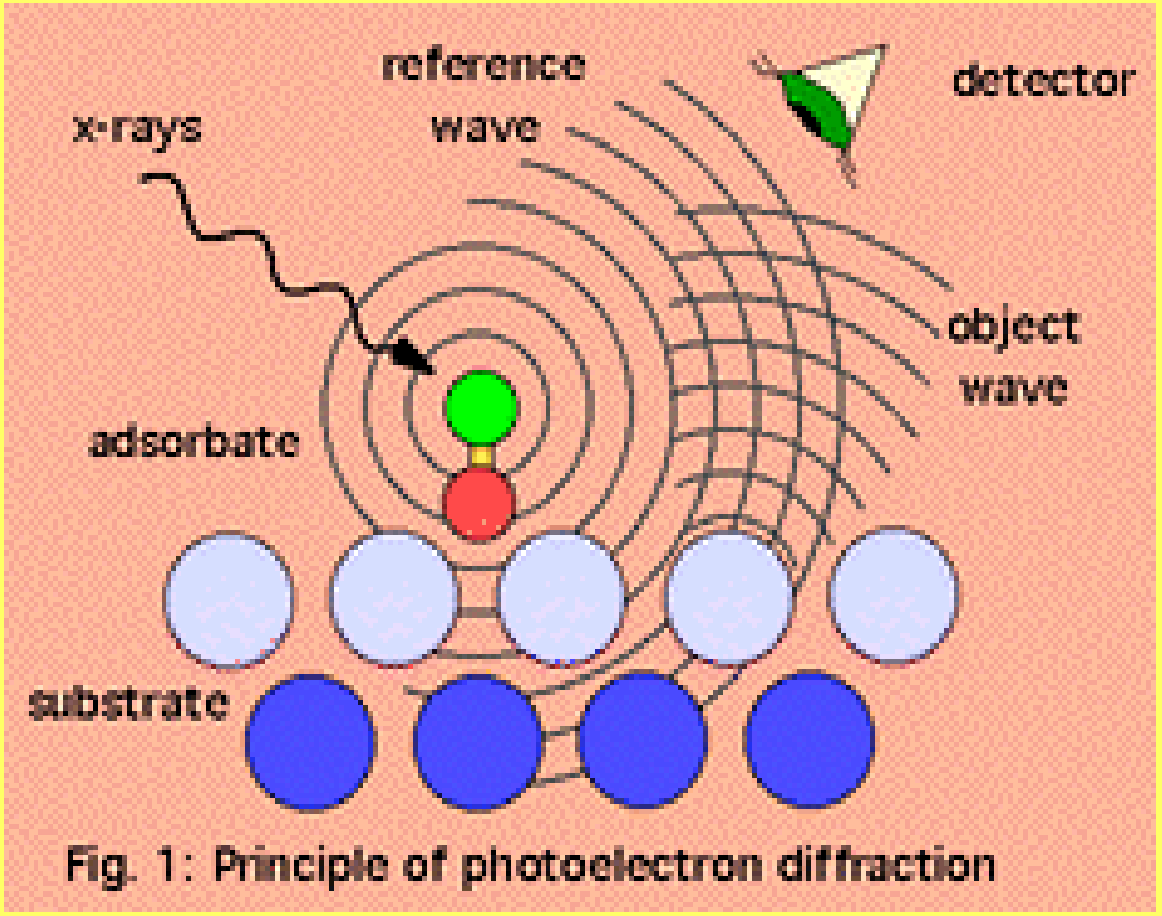

Fig. 1: Principle of photoelectron diffraction

Principio di funzionamento dell'ologramma

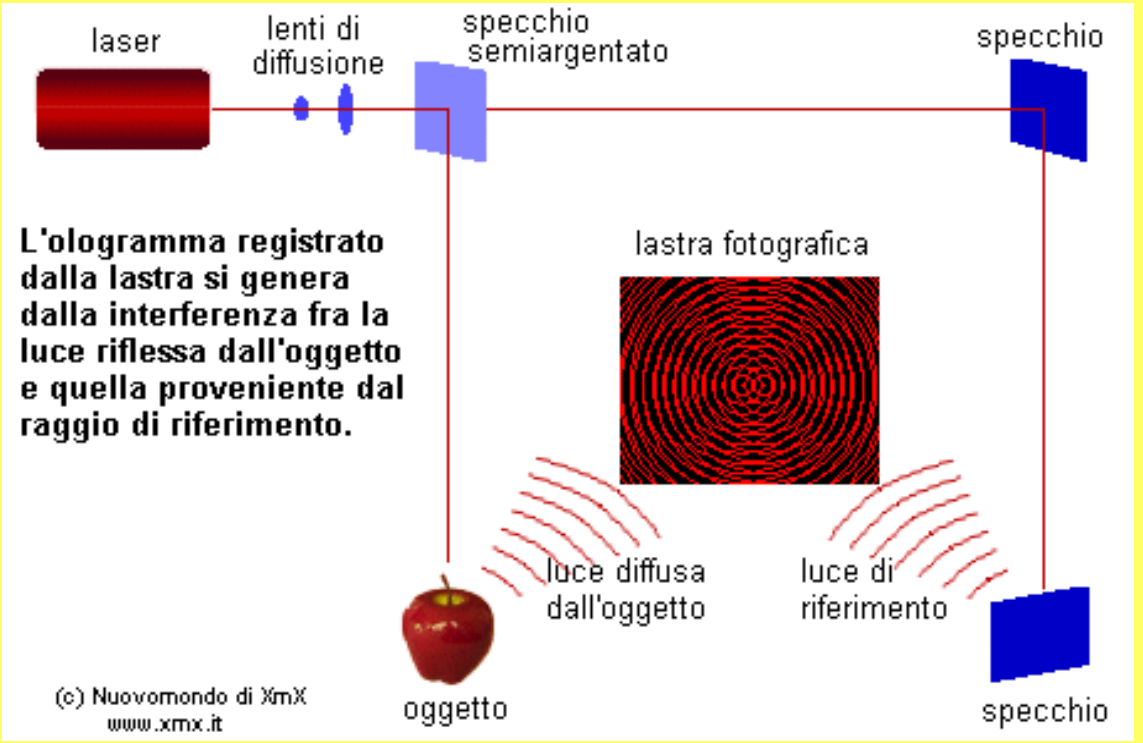

$$I = |A_0 + A_s|^2 = |A_0| + 2\mathrm{Re}A_0 A_s + |A_s|^2$$

$$\simeq |A_0| + 2\mathrm{Re}A_0 A_s$$

Multiple Scattering Theory for Spectroscopies; Sébilleau, D., Hatada, K., Ebert, H., Eds.; Springer International Publishing: Berlin/Heidelberg, Germany, 2018; Volume 204

Chapter 18
3D Atomic Structure Analysis Around Local Active Atoms by Two-Dimensional Photoelectron Diffraction and Holography

Hiroshi Daimon

H. Daimon, Phys. Rev. Lett. 86, 2034 (2001)
A. Szöke, A.I.P. Conf. Proc. 147, 361 (1986)
T. Matsushita, A. Yoshigoe, A. Agui, Europhys. Lett. 71, 597 (2005)

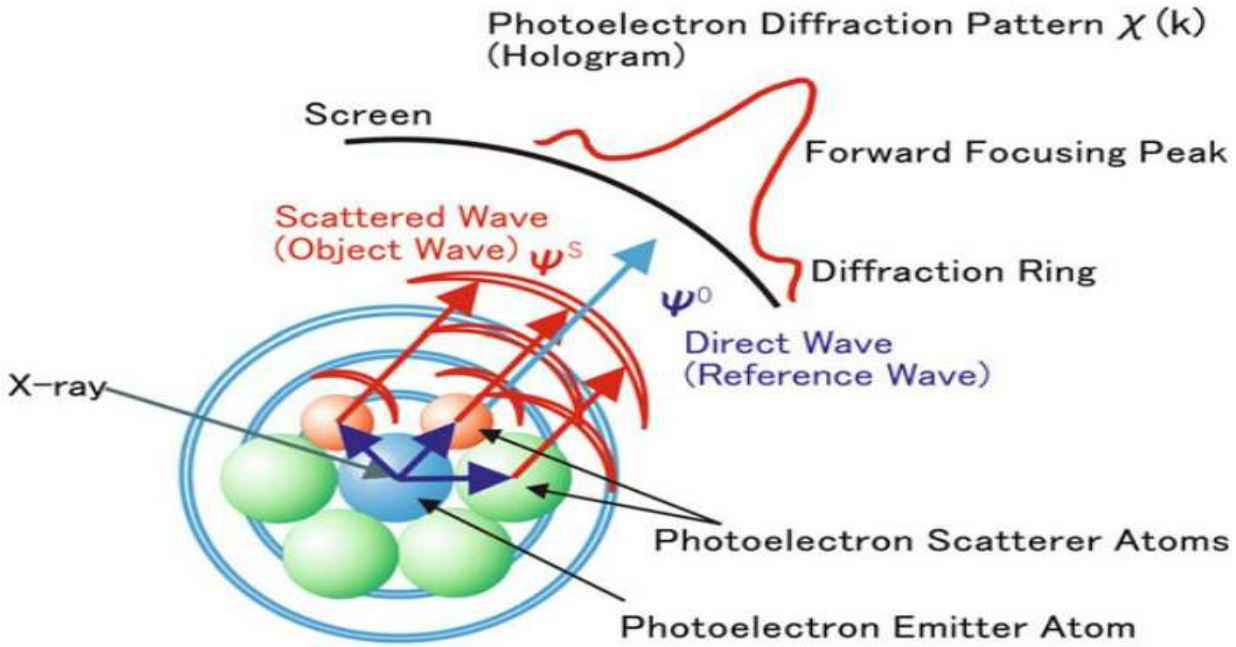

Fig. 18.1 Photoelectron diffraction and holography

$$\mu(\omega) = \sum_k \int d\omega' \, A_k(\omega') \, \mu_k^0(\omega - \omega')$$

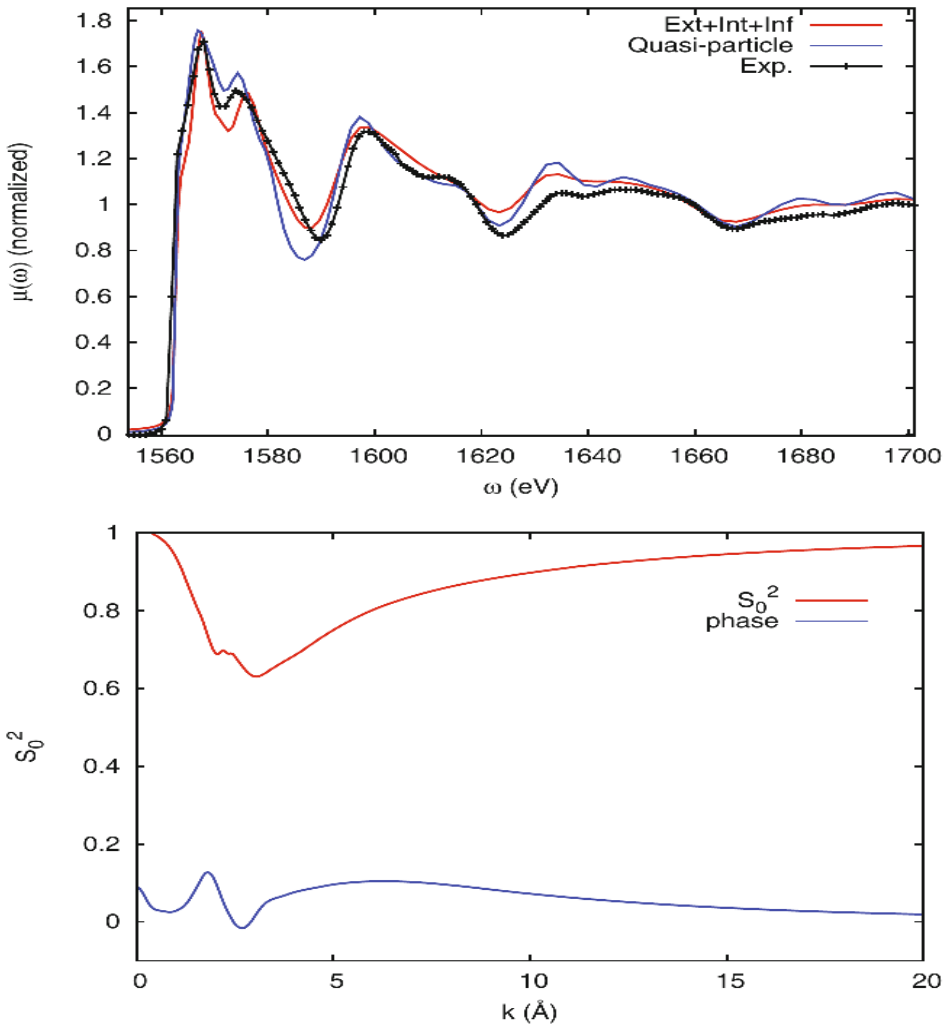

Fig. 27.1 (*top*) Theoretical Al K-edge XAS spectrum compared to the quasi-particle theory in this work and experimental data [17]; and (*bottom*) the many-body amplitude factor for the first shell R including extrinsic losses $|\bar{S}_0^2| = |S_0^2(R)|e^{-2R/\lambda_k}$ as well as the associated phase ψ_k in radians. The top figure was adapted from that in [5]

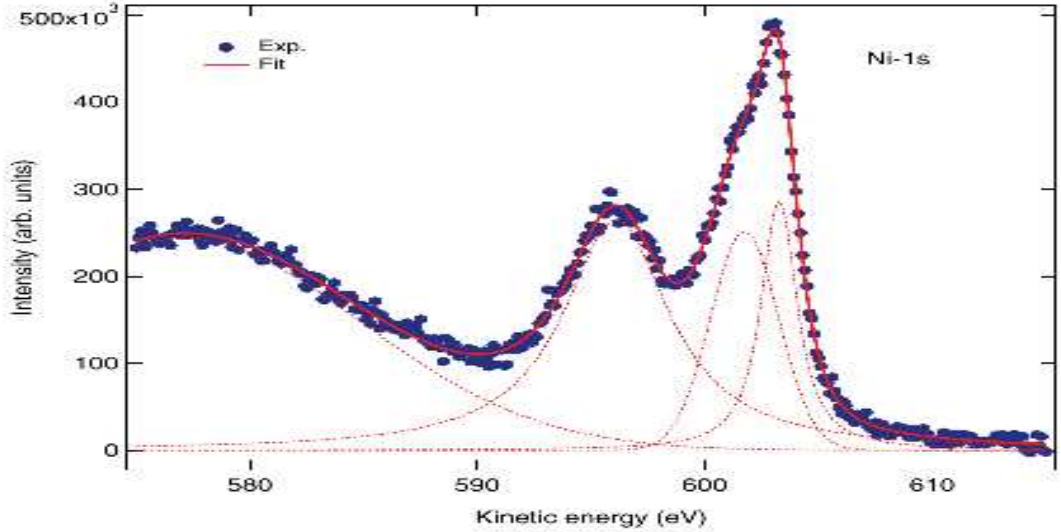

FIG. 1. (Color online) Experimental (circle) and fitted (lines) 1*s* photoemission spectra in NiO.

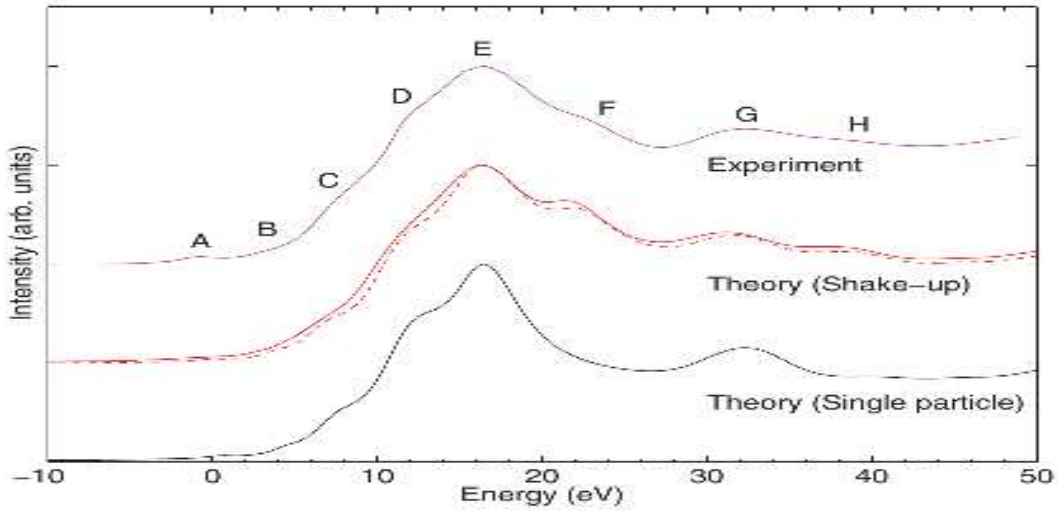

FIG. 2. (Color online) Convolution of experimental XPS (this work) and single-particle XAS calculation in NiO at the Ni *K* edge. Convolution with two or three components is shown with solid line and dashed line, respectively (middle spectra). Experimental XAS data are from Ref. 36.

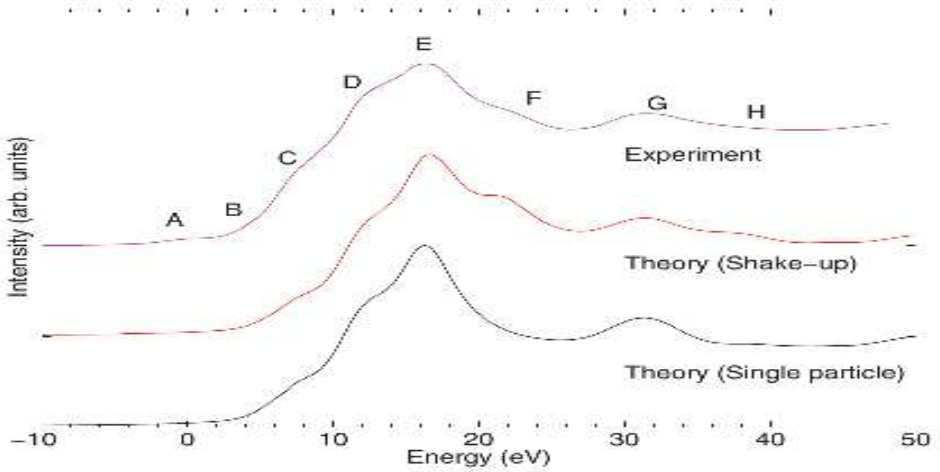

FIG. 3. (Color online) Convolution of experimental XPS data of Refs. 38 and 41 and single-particle XAS calculation in CoO at the Co K edge. Experimental XAS data are from Ref. 37.

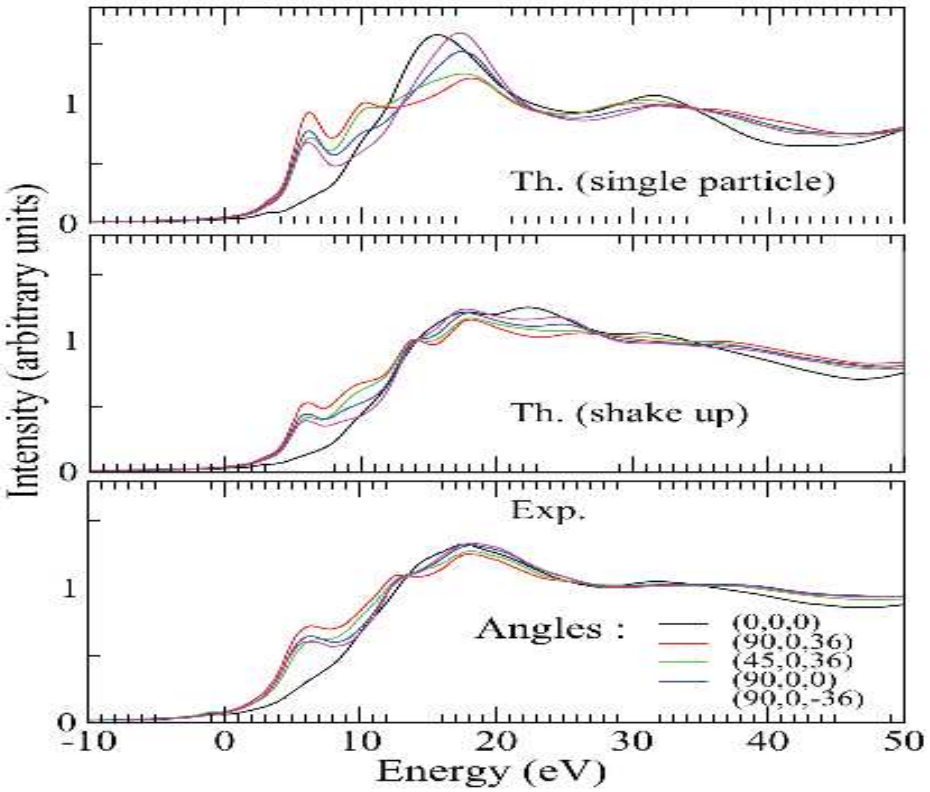

FIG. 4. (Color online) Convolution between measured XPS from Ref. 44 and single-particle XAS calculation at the Cu K edge. Experimental XAS data are from Refs. 42 and 43.

Integrating PED over emission angles: Interacting Particles

By integrating over all emission angle and photoelectron energies at fixed incoming photon energy we meausre the total absorption coefficient at that photon energy

Integrating PED over emission angles: Independent Particle Approximation

By integrate over all emission angles at a fixed electron kinetic energy we have a measure of the number of created core holes and therefore of the number of photo-emission events. This number is proportional to the absorption coefficient at the chosen energy, as born out by the mathematical derivation in the framework of MST.

In both cases the integration process eliminates the physical detector located outside the sample and replaces it with the atomic emitter (since we count the number of holes), which becomes in this way both the source and the detector of the photo-electrons.

MATTER-RADIATION INTERACTION

D. Sebilleau *et al* J. Phys.: Condens. Matter 18 R175 2006

Multiple Scattering Theory for Spectroscopies; **Sébilleau, D., Hatada, K., Ebert, H., Eds.; Springer International Publishing: Berlin/Heidelberg, Germany, 2018; Volume 204**

Definition of cross-section: Transition probability per unit time divided by the incident flux

$$\frac{v}{V}\sigma = w_{f|i}$$

$$W_{i\to f} = \frac{2\pi}{\hbar}\left|< \Phi_f|T_I|\Phi_i >\right|^2 \rho(\mathcal{E}_f)$$

Definition of the absorption coefficient

$$\frac{dN}{dx} = -Nn\sigma \ \rightarrow N = N_0\, e^{-\mu x}$$

where n is the number of absorbing centers (molecules) per unit volume and $\mu = n\sigma$

General expression of the cross-section

$$H = H_P + H_M + V_I = H_o + V_I$$

Eigenstates of the unperturbed hamiltonian H_o

$$|\Phi> = |\varphi_p> |\phi_m>$$

where E_F is determined by

$$\begin{cases} H_o|\Phi_i> = \mathcal{E}_i|\Phi_i> \quad \text{with} \quad \mathcal{E}_i = \mathsf{E}_i + E_i \\ H_o|\Phi_f> = \mathcal{E}_f|\Phi_f> \quad \text{with} \quad \mathcal{E}_f = \mathsf{E}_f + E_f \end{cases}$$

Transition probability per unit time

$$W_{i\to f} = \frac{2\pi}{\hbar} \left| < \Phi_f | T_I | \Phi_i > \right|^2 \rho(\mathcal{E}_f)$$

Expression for Transition Operator T_I

$$T_I = V_I + V_I G(\mathcal{E}_i) V_I$$

where the Resolvent $G(\mathcal{E}_i)$ is given by

$$G(\mathcal{E}_i) = \lim_{\epsilon \to 0^+} \frac{1}{\mathcal{E}_i - H + i\epsilon}$$

$$G(\mathcal{E}_i)|\Psi_n > = \frac{|\Psi_n >}{\mathcal{E}_i - \mathcal{E}_n}$$

To second order in V_I

$$T_I \approx V_I + V_I G_o(\mathcal{E}_i) V_I$$

Cross-section for incoming photons

$$V_I = \frac{e}{m}\vec{\mathbf{A}} \cdot \vec{\mathbf{p}} + \frac{e^2}{2m}\vec{\mathbf{A}}^2$$

$$\vec{\mathbf{A}}(\vec{\mathbf{r}}) = \sum_{\vec{\mathbf{q}},\hat{\mathbf{e}}_{\vec{\mathbf{q}}}} \sqrt{\frac{\hbar}{2\epsilon_0 \omega_{\vec{\mathbf{q}}} V}} \left[a_{\vec{\mathbf{q}},\hat{\mathbf{e}}_{\vec{\mathbf{q}}}} e^{i\vec{\mathbf{q}}\cdot\vec{\mathbf{r}}} \hat{\mathbf{e}}_{\vec{\mathbf{q}}} + a^{\dagger}_{\vec{\mathbf{q}},\hat{\mathbf{e}}_{\vec{\mathbf{q}}}} e^{-i\vec{\mathbf{q}}\cdot\vec{\mathbf{r}}} \hat{\mathbf{e}}^{*}_{\vec{\mathbf{q}}} \right]$$

$$T_I^{(2)} = \frac{e}{m}\vec{\mathbf{A}} \cdot \vec{\mathbf{p}} + \left(\frac{e}{m}\right)^2 \left[\frac{m}{2}\vec{\mathbf{A}} \cdot \vec{\mathbf{A}} + \vec{\mathbf{A}} \cdot \vec{\mathbf{p}}\, G_o(\mathcal{E}_i)\, \vec{\mathbf{A}} \cdot \vec{\mathbf{p}} \right] + \mathcal{O}(\frac{e^3}{m^3})$$

For photo-absorption

$$T_I^{\text{abs}} = \frac{e}{m} \sum_{\vec{\mathbf{q}}, \hat{\mathbf{e}}_{\vec{\mathbf{q}}}} \sqrt{\frac{\hbar}{2\epsilon_o \omega_{\vec{\mathbf{q}}} V}} \, (\hat{\mathbf{e}}_{\vec{\mathbf{q}}} \cdot \vec{\mathbf{p}}) \, a_{\vec{\mathbf{q}}, \hat{\mathbf{e}}_{\vec{\mathbf{q}}}} \, e^{i\vec{\mathbf{q}} \cdot \vec{\mathbf{r}}}$$

The photo-absorption cross-section is obtained by dividing the t.p. per unit time $W_{i \to f}$ by the incident photon flux $I_P = c/V$

$$\sigma_{abs} = 4\pi^2 \alpha \frac{\hbar}{m^2 \omega_{\vec{\mathbf{q}}}} \sum_f \left| < \phi_f | \hat{\mathbf{e}}_{\vec{\mathbf{q}}} \cdot \vec{\mathbf{p}} \, e^{i\vec{\mathbf{q}} \cdot \vec{\mathbf{r}}} | \phi_i > \right|^2 \delta(E_i - E_f + \hbar\omega_{\vec{\mathbf{q}}})$$

Using

$$< \phi_n | \hat{\mathbf{e}}_{\vec{\mathbf{q}}} \cdot \vec{\mathbf{p}} | \phi_m > = \, im \, \omega_{\vec{\mathbf{q}}} \, < \phi_n | \hat{\mathbf{e}}_{\vec{\mathbf{q}}} \cdot \vec{\mathbf{r}} | \phi_m >$$

we finally get

$$\sigma_{abs} = 4\pi^2 \alpha \, \hbar\omega_{\vec{\mathbf{q}}} \sum_f \left| < \phi_f | \hat{\mathbf{e}}_{\vec{\mathbf{q}}} \cdot \vec{\mathbf{r}} | \phi_i > \right|^2 \delta(E_i - E_f + \hbar\omega_{\vec{\mathbf{q}}})$$

Photoemission cross-section: Many body

$$\frac{d\sigma(\omega)}{d\hat{\mathbf{k}}} = 4\pi^2\alpha\,\hbar\omega \left| < \Theta\Psi^N_{\vec{\mathbf{k}}} | \vec{\mathbf{e}} \cdot \sum_{i=1}^{n} \vec{\mathbf{r}}_i | \Psi^N_g > \right|^2$$

Photoemission cross-section: Independent Particle Approach

$$\frac{d\sigma}{d\hat{k}} = 4\pi^2\alpha\hbar\omega | < \psi^-_{\mathbf{k}}(\mathbf{r}) | \boldsymbol{\epsilon} \cdot \mathbf{r} | \phi_c > |^2$$

Scattering processes a): Thomson scattering

$$< \Phi_f | T^{(2)}_{I\,(a)} | \Phi_i > = \frac{e^2}{2m} \frac{\hbar}{2\epsilon_o V} \frac{1}{\sqrt{\omega_{\vec{\mathbf{q}}_f} \omega_{\vec{\mathbf{q}}_i}}} < \Phi_f | (\hat{\mathbf{e}}^*_{\vec{\mathbf{q}}_f} \cdot \hat{\mathbf{e}}_{\vec{\mathbf{q}}_i}) e^{i(\vec{\mathbf{q}}_i - \vec{\mathbf{q}}_f)\cdot\vec{\mathbf{r}}}$$

$$\times \left[a_{\vec{\mathbf{q}}_i \hat{\mathbf{e}}_{\vec{\mathbf{q}}_i}} a^\dagger_{\vec{\mathbf{q}}_f \hat{\mathbf{e}}_{\vec{\mathbf{q}}_f}} + a^\dagger_{\vec{\mathbf{q}}_f \hat{\mathbf{e}}_{\vec{\mathbf{q}}_f}} a_{\vec{\mathbf{q}}_i \hat{\mathbf{e}}_{\vec{\mathbf{q}}_i}} \right] | \Phi_i >$$

Scattering processes b) and c): Resonant and non-resonant contributions

$$
\begin{cases}
< \Phi_f | T^{(2)}_{I\,(b)} | \Phi_i > &= N \sum_n \dfrac{< \phi_f | \hat{\mathbf{e}}^*_{\vec{\mathbf{q}}_f} \cdot \vec{\mathbf{p}}\, e^{-i\vec{\mathbf{q}}_f \cdot \vec{\mathbf{r}}} | \phi_n >< \phi_n | \hat{\mathbf{e}}_{\vec{\mathbf{q}}_i} \cdot \vec{\mathbf{p}}\, e^{i\vec{\mathbf{q}}_i \cdot \vec{\mathbf{r}}} | \phi_i}{E_i - E_n + \hbar\omega_{\vec{\mathbf{q}}_i} + i\epsilon} \\
< \Phi_f | T^{(2)}_{I\,(c)} | \Phi_i > &= N \sum_n \dfrac{< \phi_f | \hat{\mathbf{e}}_{\vec{\mathbf{q}}_i} \cdot \vec{\mathbf{p}}\, e^{i\vec{\mathbf{q}}_i \cdot \vec{\mathbf{r}}} | \phi_n >< \phi_n | \hat{\mathbf{e}}^*_{\vec{\mathbf{q}}_f} \cdot \vec{\mathbf{p}}\, e^{-i\vec{\mathbf{q}}_f \cdot \vec{\mathbf{r}}} | \phi_i}{E_i - E_n - \hbar\omega_{\vec{\mathbf{q}}_f} + i\epsilon} \\
N &= \left(\frac{e}{m}\right)^2 \frac{\hbar}{2\epsilon_o V} \frac{1}{\sqrt{\omega_{\vec{\mathbf{q}}_f}\omega_{\vec{\mathbf{q}}_i}}}
\end{cases}
$$

To find the Cross-section for scattering processess we need to divide by the incoming flux c/V and multiply by the photon final density of states $\frac{V}{(2\pi)^3}\frac{(\hbar\omega_{\vec{\mathbf{q}}_f})^2}{\hbar^3 c^3}$

Cross-section for scattering processes with $\vec{\mathbf{Q}} = \vec{\mathbf{q}}_f - \vec{\mathbf{q}}_i$

$$\frac{d\sigma}{d\Omega} = r_o^2 \frac{\omega_{\vec{\mathbf{q}}_f}}{\omega_{\vec{\mathbf{q}}_i}} \left| \hat{\mathbf{e}}^*_{\vec{\mathbf{q}}_f} \cdot \hat{\mathbf{e}}_{\vec{\mathbf{q}}_i} < \phi_f | \, e^{-i\vec{\mathbf{Q}}\cdot\vec{\mathbf{r}}} \, | \phi_i > \right.$$

$$\left. \frac{1}{m} \left[\sum_n \frac{< \phi_f | \hat{\mathbf{e}}^*_{\vec{\mathbf{q}}_f} \cdot \vec{\mathbf{p}} \, e^{-i\vec{\mathbf{q}}_f\cdot\vec{\mathbf{r}}} | \phi_n >< \phi_n | \hat{\mathbf{e}}_{\vec{\mathbf{q}}_i} \cdot \vec{\mathbf{p}} \, e^{i\vec{\mathbf{q}}_i\cdot\vec{\mathbf{r}}} | \phi_i >}{E_i - E_n + \hbar\omega_{\vec{\mathbf{q}}_i} + i\epsilon} \right. \right.$$

$$\left. \left. + \frac{< \phi_f | \hat{\mathbf{e}}_{\vec{\mathbf{q}}_i} \cdot \vec{\mathbf{p}} \, e^{i\vec{\mathbf{q}}_i\cdot\vec{\mathbf{r}}} | \phi_n >< \phi_n | \hat{\mathbf{e}}^*_{\vec{\mathbf{q}}_f} \cdot \vec{\mathbf{p}} \, e^{-i\vec{\mathbf{q}}_f\cdot\vec{\mathbf{r}}} | \phi_i >}{E_i - E_n - \hbar\omega_{\vec{\mathbf{q}}_f} + i\epsilon} \right] \right|^2$$

where $r_o = e^2/(4\pi\epsilon_0 mc^2)$ is the classical electron radius

In the case of elastic scattering and resonant conditions, putting $f_T(\vec{\mathbf{Q}}) = \int |\rho(\vec{\mathbf{r}})| e^{-i\vec{\mathbf{Q}}\cdot\vec{\mathbf{r}}} d\vec{\mathbf{r}}$ and $\vec{\mathbf{Q}} = \vec{\mathbf{q}}_f - \vec{\mathbf{q}}_i$

$$\frac{d\sigma}{d\Omega} = r_o^2 \left| \hat{\mathbf{e}}^*_{\vec{\mathbf{q}}_f} \cdot \hat{\mathbf{e}}_{\vec{\mathbf{q}}_i} f_T(\vec{\mathbf{Q}}) + \frac{1}{m} \sum_n \frac{< \phi_i | \hat{\mathbf{e}}^*_{\vec{\mathbf{q}}_f} \cdot \vec{\mathbf{p}}\, e^{-i\vec{\mathbf{q}}_f\cdot\vec{\mathbf{r}}} | \phi_n >< \phi_n | \hat{\mathbf{e}}_{\vec{\mathbf{q}}_i} \cdot \vec{\mathbf{p}}\, e^{i\vec{\mathbf{q}}_i\cdot\vec{\mathbf{r}}} | \phi_i >}{E_i - E_n + \hbar\omega_{\vec{\mathbf{q}}_i} + i\epsilon} \right|^2$$

$$\frac{d\sigma}{d\Omega} = r_o^2 \left| \hat{\mathbf{e}}^*_{\vec{\mathbf{q}}_f} \cdot \hat{\mathbf{e}}_{\vec{\mathbf{q}}_i} f_T(\vec{\mathbf{Q}}) + f'(\hbar\omega_{\vec{\mathbf{q}}_i}) + i f''(\hbar\omega_{\vec{\mathbf{q}}_i}) \right|^2$$

$$f''(\hbar\omega_{\vec{\mathbf{q}}_i}) = -\frac{\pi}{m} \sum_n < \phi_i | \hat{\mathbf{e}}^*_{\vec{\mathbf{q}}_f} \cdot \vec{\mathbf{p}}\, e^{-i\vec{\mathbf{q}}_f\cdot\vec{\mathbf{r}}} | \phi_n >< \phi_n | \hat{\mathbf{e}}_{\vec{\mathbf{q}}_i} \cdot \vec{\mathbf{p}}\, e^{i\vec{\mathbf{q}}_i\cdot\vec{\mathbf{r}}} | \phi_i > \delta(E_i - E_n + \hbar\omega_{\vec{\mathbf{q}}_i})$$

Writing $\vec{\mathrm{r}} = \vec{\mathrm{r}}_k + \vec{\mathrm{R}}_k$ we find

$$\frac{d\sigma}{d\Omega} = r_o^2 \left| \hat{\mathbf{e}}^*_{\vec{\mathbf{q}}_f} \cdot \hat{\mathbf{e}}_{\vec{\mathbf{q}}_i} \, f_T^k(\vec{\mathbf{Q}}) + \right.$$

$$\left. \frac{1}{m} \sum_n \frac{< \phi_i | \hat{\mathbf{e}}^*_{\vec{\mathbf{q}}_f} \cdot \vec{\mathbf{p}} \, e^{-i\vec{\mathbf{q}}_f \cdot \vec{\mathbf{r}}_k} | \phi_n > < \phi_n | \hat{\mathbf{e}}_{\vec{\mathbf{q}}_i} \cdot \vec{\mathbf{p}} \, e^{i\vec{\mathbf{q}}_i \cdot \vec{\mathbf{r}}_k} | \phi_i >}{E_i - E_n + \hbar\omega_{\vec{\mathbf{q}}_i} + i\epsilon} \right|^2$$

$$\left| \sum_k e^{-i\vec{\mathbf{Q}} \cdot \vec{\mathbf{R}}_k} \right|^2$$

In the case of many atoms per unit cell at positions ρ_j the structure factor is given by

$$F(\vec{\mathbf{Q}}, \hbar\omega) = \sum_j \mathrm{e}^{-\mathrm{i}\tilde{\mathbf{Q}} \cdot \tilde{\rho}_\mathrm{j}} \, \mathrm{f}_\mathrm{j}(\omega)$$

REXS: Resonant Elastic X-ray Scattering

$$\frac{\mathrm{d}\sigma}{\mathrm{d}\Omega} = r_o^2 \left| \hat{\mathbf{e}}^*_{\mathbf{q_f}} \cdot \hat{\mathbf{e}}_{\mathbf{q_i}} \, f_T(\mathbf{Q}) + \right.$$

$$\left. \frac{1}{m} \sum_n \frac{\langle \phi_i | \hat{\mathbf{e}}^*_{\mathbf{q_f}} \cdot \mathbf{p} \, \mathrm{e}^{-\mathrm{i}\mathbf{q_f}\cdot\mathbf{r}} | \phi_\mathbf{n} \rangle \langle \phi_\mathbf{n} | \hat{\mathbf{e}}_{\mathbf{q_i}} \cdot \mathbf{p} \, \mathrm{e}^{\mathrm{i}\mathbf{q_i}\cdot\mathbf{r}} | \phi_\mathbf{i} \rangle}{E_i - E_n + \hbar\omega_{\mathbf{q_i}} - \mathrm{i}\Gamma_n} \right|^2$$

$$\frac{\mathrm{d}\sigma}{\mathrm{d}\Omega} = r_o^2 \left| \hat{\mathbf{e}}^*_{\mathbf{q_f}} \cdot \hat{\mathbf{e}}_{\mathbf{q_i}} \, f_T(\mathbf{Q}) + \mathbf{f}'(\hbar\omega_{\mathbf{q_i}}) + \mathrm{i}\mathbf{f}''(\hbar\omega_{\mathbf{q_i}}) \right|^2$$

$$f_j''(E) = \frac{r_0}{m} \sum_{LL'} \langle \phi_i^{(j)} | \hat{\mathbf{e}}^*_{\mathbf{q_s}} \cdot \mathbf{p} \, \mathrm{e}^{-\mathrm{i}\mathbf{q_s}\cdot\mathbf{r}} | \tilde{\mathbf{\Phi}}_\mathbf{L}(\mathbf{r_j}; \mathbf{E}) \rangle \langle \tilde{\mathbf{\Phi}}_{\mathbf{L'}}(\mathbf{r_j}; \mathbf{E}) | \hat{\mathbf{e}}_{\mathbf{q_i}} \cdot \mathbf{p} \, \mathrm{e}^{\mathrm{i}\mathbf{q_i}\cdot\mathbf{r}} | \phi_\mathbf{i}^{(\mathbf{j})} \rangle$$

$$\times \quad (-\frac{1}{\pi}) \, \Im \left[\tau^{jj}_{LL'}(E) - T^{jj}_{LL'}(E) \right]$$

$$f_j(\omega) = \int_0^\infty dE \, \frac{f_j''(E)}{\hbar\omega - (E + I_c) - \mathrm{i}\Gamma(E)}$$

LEED: Low-Energy Electron Diffraction

$$\frac{\mathrm{d}\sigma}{\mathrm{d}\hat{\mathbf{k}}_s} = (4\pi)^2 \left| \sum_{i,L} \sum_{j,L'} \mathrm{i}^{-l'} Y_{L'}(\hat{\mathbf{k}}_s)\, \mathrm{e}^{\mathrm{i}\mathbf{k}_s \cdot \mathbf{R}_{ij}}\, \tau^{ji}_{L'L}\, \mathrm{i}^{l} Y_L(\hat{\mathbf{k}}_i) \mathrm{e}^{-\mathrm{i}\mathbf{q}\cdot\mathbf{R}_{io}} \right|^2$$

EELS: Electron Energy Loss Spectroscopy

$$\frac{\mathrm{d}\sigma}{\mathrm{d}\hat{\mathbf{k}}_f} = -4\pi^3 \frac{k_f}{k_i} \sum_{m_o} \sum_{L,L'} \Im \left[M^*_{L_o L}\, \tau^{00}_{LL'}\, M_{L' L_o} \right]$$

$$M_{LL_o} = \int \tilde{\Phi}_L(\mathbf{r}) \mathbf{T}(\mathbf{r}) \phi_{\mathbf{L_o}}(\mathbf{r})\, \mathrm{d}\mathbf{r}$$

$$T^{\pm}(\mathbf{r}) = \int \phi^{-}_{\mathbf{f}}{}^{*}(\mathbf{r}') \left(\frac{\mathbf{1}}{|\mathbf{r}-\mathbf{r}'|} \pm \frac{4\pi}{|\mathbf{k_i}-\mathbf{k}|} \delta(\mathbf{r}-\mathbf{r}') \right) \phi^{+}_{\mathbf{i}}(\mathbf{r}')\, \mathrm{d}\mathbf{r}'$$

MULTIPLE SCATTERING THEORY

From Dyson equation (with complex self-energy)

$$\left[\nabla^2 + E - V_c(\mathbf{r}) - \Sigma(\mathbf{r}; E)\right] \psi(\mathbf{r}) = 0$$

with boundary conditions

$$\psi(\mathbf{r}; \mathbf{k}) \simeq \left(\frac{k}{16\pi^3}\right)^{\frac{1}{2}} \left[\mathrm{e}^{\mathrm{i}\mathbf{k}\cdot\mathbf{r}} + f(\hat{\mathbf{r}}; \mathbf{k}) \frac{\mathrm{e}^{\mathrm{i}kr}}{r}\right]$$

introducing $G_0^+(\mathbf{r} - \mathbf{r}')$

$$\left[\nabla^2 + E\right] G_0^+(\mathbf{r} - \mathbf{r}') = \delta(\mathbf{r} - \mathbf{r}')$$

we get THE LIPPMANN-SCHWINGER equation

$$\psi(\mathbf{r}; \mathbf{k}) = \mathrm{e}^{\mathrm{i}\mathbf{k}\cdot\mathbf{r}} + \int G_0^+(\mathbf{r} - \mathbf{r}')\, V(\mathbf{r}'; E)\, \psi(\mathbf{r}'; \mathbf{k})\, \mathrm{d}^3\mathrm{r}'$$

Remembering the expansions

$$
\begin{aligned}
\mathrm{e}^{\mathrm{i}\mathbf{k}\cdot\mathbf{r}} &= 4\pi \sum_L i^l Y_L(\hat{\mathbf{k}}) J_L(\mathbf{r};k) \\
G_0^+(\mathbf{r}-\mathbf{r}';E) &= \sum_L J_L(\mathbf{r};k)\tilde{H}_L^+(\mathbf{r}';k) \ (r<r') \\
&= \sum_L J_L(\mathbf{r}';k)\tilde{H}_L^+(\mathbf{r};k) \ (r>r')
\end{aligned}
$$

and putting

$$\psi(\mathbf{r}) = \sum_L A_L(\mathbf{k})\psi_L(\mathbf{r})$$

$$A_L = 4\pi i^l Y_L(\hat{\mathbf{k}})$$

we find

$$\psi_L(\mathbf{r};k) = J_L(\mathbf{r};k) + \int G_0^+(\mathbf{r}-\mathbf{r}';k)\, V(\mathbf{r}')\, \psi_L(\mathbf{r}';k)\, \mathrm{d}^3\mathrm{r}'$$

MT approximation (MXAN)

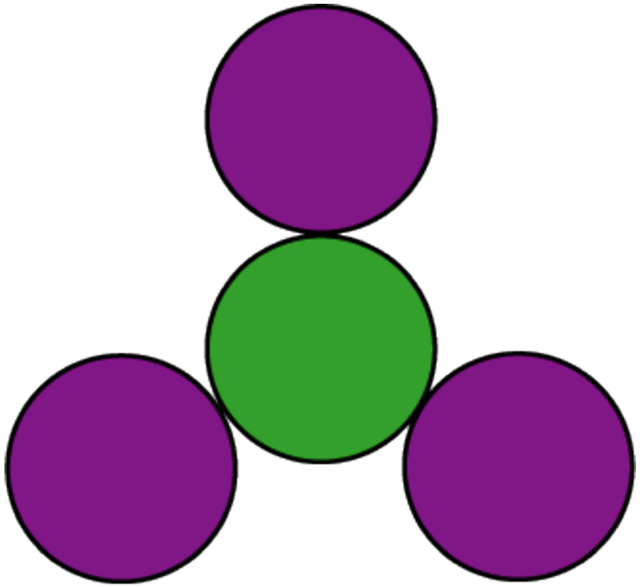

Use spherical shaped and averaged potential

outside the cells potential is flat

Non-MT (FPMS)

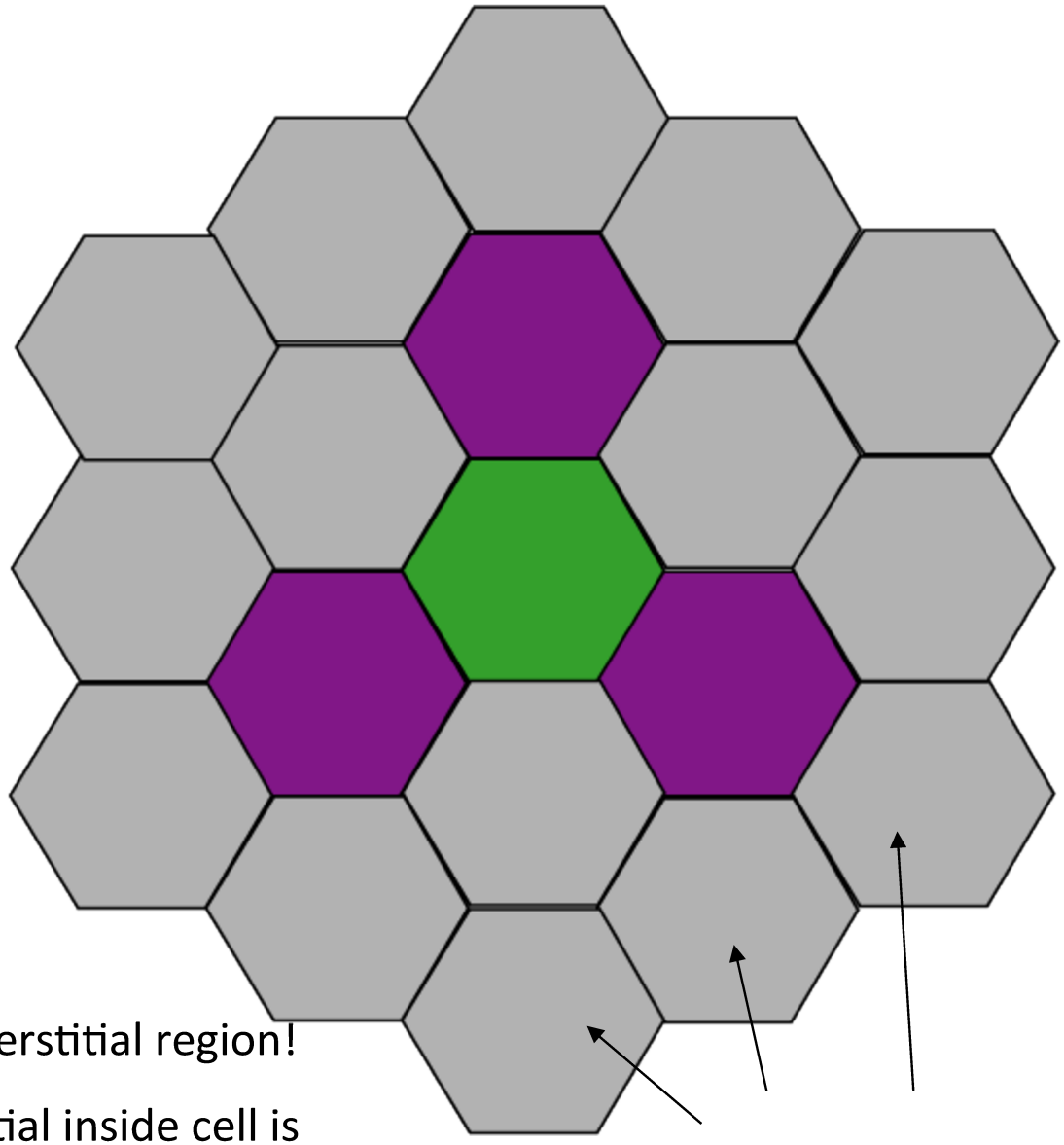

No interstitial region!

Potential inside cell is anisotropic

Empty Cells (EC)

At great distances

$$\begin{aligned}\psi_L(\mathbf{r};\mathbf{k}) &= J_L(\mathbf{r};k) + \sum_{L'} \tilde{H}^+_{L'}(\mathbf{r};k) \int J_{L'}(\mathbf{r}';k)\, V(\mathbf{r}')\, \psi_L(\mathbf{r}';k)\, \mathrm{d}^3\mathrm{r}' \\ &= J_L(\mathbf{r};k) + \sum_{L'} \tilde{H}^+_{L'}(\mathbf{r};k)\, T_{L'L}\end{aligned}$$

Defining

$$T_{L'L} = \int J_{L'}(\mathbf{r};k)\, V(\mathbf{r})\, \psi_L(\mathbf{r};k)\, \mathrm{d}^3\mathrm{r}$$

Partition the space in cells Ω_j - Introduce local solutions

$$\psi_L(\mathbf{r}_j;k) = J_L(\mathbf{r}_j;k) + \int_{\Omega_j} G^+_0(\mathbf{r}_j - \mathbf{r}'_j;k)\, v_j(\mathbf{r}'_j)\, \psi_L(\mathbf{r}'_j;k)\, \mathrm{d}^3\mathrm{r}'_\mathrm{j}$$

THEN THE GLOBAL SOLUTION CAN BE EXPRESSED LOCALLY AS

$$\psi(\mathbf{r}_j;\mathbf{k}) = \sum_L C^j_L(\mathbf{k}) \psi_L(\mathbf{r}_j;k)$$

Referring to center R_i ($\mathrm{r}_i = \mathrm{r} - \mathrm{R}_i$)

$$\begin{aligned}\psi(\mathbf{r}_i;\mathbf{k}) &= \mathrm{e}^{\mathrm{i}\mathbf{k}\cdot\mathbf{r}_i}\,\mathrm{e}^{\mathrm{i}\mathbf{k}\cdot\mathbf{R}_i} \\ &+ \int_{\Omega_i} G_0^+(\mathbf{r}_i - \mathbf{r}_i';k)\, v_i(\mathbf{r}_i')\, \psi(\mathbf{r}_i';\mathbf{k})\, \mathrm{d}^3\mathrm{r}_\mathrm{i}' \\ &+ \sum_{j\neq i} \int_{\Omega_j} G_0^+(\mathbf{r}_j - \mathbf{r}_j';k)\, v_j(\mathbf{r}_j')\, \psi(\mathbf{r}_j';\mathbf{k})\, \mathrm{d}^3\mathrm{r}_\mathrm{j}'\end{aligned}$$

Using the local representation we obtain

$$\begin{aligned}\sum_L C_L^i(\mathbf{k})\, J_L(\mathbf{r}_i;k) &= \mathrm{e}^{\mathrm{i}\mathbf{k}\cdot\mathbf{r}_i}\,\mathrm{e}^{\mathrm{i}\mathbf{k}\cdot\mathbf{R}_i} \\ &+ \sum_{j\neq i} \int_{\Omega_j} G_0^+(\mathbf{r}_j - \mathbf{r}_j';k)\, v_j(\mathbf{r}_j') \sum_L C_L^j(\mathbf{k})\psi_L(\mathbf{r}_j';k)\, \mathrm{d}^3\end{aligned}$$

We use the two center expansion for $G_0^+(\mathrm{r} - \mathrm{r}';k)$

$$G_0^+(\mathbf{r} - \mathbf{r}';k) = \sum_{LL'} J_L(\mathbf{r}_i;k)\, G_{LL'}^{ij}\, J_L(\mathbf{r}_j;k)$$

where $G^{ij}_{LL'}$ are the KKR structure factors

$$G^{ij}_{LL'} = 4\pi \sum_{L''} C(L, L'; L'')\, i^{l-l'+l''}\, \tilde{H}^{+}_{L''}(\mathbf{R}_{ij}; k)$$

with

$$C(L, L'; L'') = \int Y_L(\Omega) Y_{L'}(\Omega) Y_{L''}(\Omega) \mathrm{d}\Omega$$

Finally for the amplitudes $C^i_L(\mathrm{k})$ we find

$$C^i_L(\mathbf{k}) = I^i_L(\mathbf{k}) + \sum_{j \neq i} \sum_{L'L''} G^{ij}_{LL'}\, T^j_{L'L''}\, C^j_{L''}(\mathbf{k})$$

with

$$I^i_L(\mathbf{k}) = \sqrt{\frac{k}{\pi}}\, i^l Y_L(\hat{\mathbf{k}}) \mathrm{e}^{\mathrm{i}\mathbf{k}\cdot\mathbf{R}_i}$$

Introduce the local scattering amplitudes

$$B_L^j(\mathbf{k}) = \sum_{L'} T_{LL'}^j C_{L'}^j(\mathbf{k})$$

so that

$$\psi(\mathbf{r}_j) = \sum_L B_L^j(\mathbf{k}) \Phi_L(\mathbf{r}_j)$$

The amplitudes $B_L^j(\mathbf{k})$ satisfy the MS Equations

$$\sum_{jL'} \left(T^{-1} - G\right)_{LL'}^{ij} B_{L'}^j(\mathbf{k}) = I_L^i(\mathbf{k})$$

In the case of periodic systems

$$\sum_{jL'} \left(T^{-1} - G(\mathbf{k}_{\mathsf{BZ}}; E)\right)_{LL'} B_{L'}(\mathbf{k}_{\mathsf{BZ}}) = 0$$

Introducing the scattering path operator

$$\tau^{ij}_{LL'} = \left[\left(\mathbf{T}^{-1} - \mathbf{G}\right)^{-1}\right]^{ij}_{LL'} = \left[\sum_n (\mathbf{TG})^n \mathbf{T}\right]^{ij}_{LL'} = \left[\sum_n \mathbf{T}\,(\mathbf{GT})^n\right]^{ij}_{LL'}$$

we have the solution

$$B^o_L(\mathbf{k}) = \sum_{jL'} \tau^{oj}_{LL'} i^{l'} Y_{L'}(\hat{\mathbf{k}}) \mathrm{e}^{\mathrm{i}\mathbf{k}\cdot\mathbf{R}_{jo}} (k/\pi)^{1/2}$$

Generalized optical theorem for real potentials and projected density of states

$$\int \mathrm{d}\hat{\mathbf{k}} \left[B^i_L(\mathbf{k})\right]^* B^j_{L'}(\mathbf{k}) = -\frac{1}{\pi} \Im \left[\tau^{ij}_{LL'}\right]$$

Photoemission cross-section

$$\frac{d\sigma}{d\hat{k}} = 4\pi^2 \alpha \hbar\omega | < \psi^-_{\mathbf{k}}(\mathbf{r}) | \boldsymbol{\epsilon}\cdot\mathbf{r} | \phi_c > |^2$$

$$\frac{d\sigma}{d\hat{\mathbf{k}}} = 4\pi^2 \alpha \hbar \omega \sum_{L_c} \left| \sum_{L} M_{L_c L} \left[B^o_L(\mathbf{k}) \right]^\star \right|^2$$

$$M_{L_c\, L}\,(E) \;=\; \int_{\Omega_o} d\,\mathbf{r}_o\, \phi^c_{L_c}(\mathbf{r}_o)\,(\boldsymbol{\epsilon}\cdot\mathbf{r}_o)\,\Phi_L(\mathbf{r}_o;k)$$

XAS: X-ray Absoprtion; real potential

$$\begin{aligned}
\sigma_{tot}(\omega) \;&=\; \int \frac{d\sigma}{d\hat{\mathbf{k}}} d\hat{\mathbf{k}} \;\propto\; \sum_{LL'} M_{L_c L} \int d\hat{\mathbf{k}}\, \left[B^o_L(\mathbf{k}) \right]^\star B^o_{L'}(\mathbf{k})\, M_{L' L_c} \\
&=\; -\frac{1}{\pi} \Im \sum_{LL'} M_{L_c L} \left[\tau^{oo}_{LL'} \right] M_{L' L_c}
\end{aligned}$$

Connection between GF and XAS

$$\left[\nabla^2 + E - V_{eff}(\mathbf{r}) \right] G^+(\mathbf{r}-\mathbf{r}';E) = \delta(\mathbf{r}-\mathbf{r}')$$

Solution: Spectral Representation

$$G(\mathbf{r},\mathbf{r}';E) = \sum_n \frac{\Phi_n(\mathbf{r})\,\Phi_n(\mathbf{r}')}{E - E_n}$$

so that

$$\Im G(\mathbf{r},\mathbf{r}';E) = -\frac{1}{\pi}\sum_n \Phi_n(\mathbf{r})\,\Phi_n(\mathbf{r}')\,\delta(E-E_n)$$

Remembering that

$$\sigma_{abs} \;=\; 4\pi^2\alpha\,\hbar\omega\,\sum_f \left|< \Phi_f|\hat{\epsilon}\cdot\vec{\mathbf{r}}|\Phi_i >\right|^2\,\delta(E_i - E_f + \hbar\omega)$$

we find

$$\sigma_{tot}(\omega) \propto -\frac{1}{\pi}\Im\int < \phi^c_{L_c}(\mathbf{r}_o)|\hat{\epsilon}\cdot\mathbf{r}|G(\mathbf{r},\mathbf{r}';E)|\hat{\epsilon}\cdot\mathbf{r}'|\phi^c_{L_c}(\mathbf{r}'_o) > \mathrm{d}\mathbf{r}\mathrm{d}\mathbf{r}'$$

Explicit solution of GF in MST

$$G(\mathbf{r},\mathbf{r}';E) = \sum_{LL'}\Phi_L(\mathbf{r}_o)\,\tau^{oo}_{LL'}\,\Phi_{L'}(\mathbf{r}'_o) - \sum_{LL'}\Phi_L(\mathbf{r}_{o<})\tilde{\Lambda}^+_L(\mathbf{r}_{o>})$$

Therefore

$$\sigma_{tot}(\omega) = -\frac{1}{\pi}\Im\sum_{LL'} M_{L_cL}\left[\tau^{oo}_{LL'}\right]M_{L'L_c}$$

$$\int \mathrm{d}\mathbf{r}\,\Im G(\mathbf{r},\mathbf{r};E) = \sum_{iL}\int_{\Omega_i}\mathrm{d}\mathbf{r}\,|\Phi^i_L(\mathbf{r}_i;k)|^2\,\Im\boldsymbol{\tau}^{ii}_{LL}$$

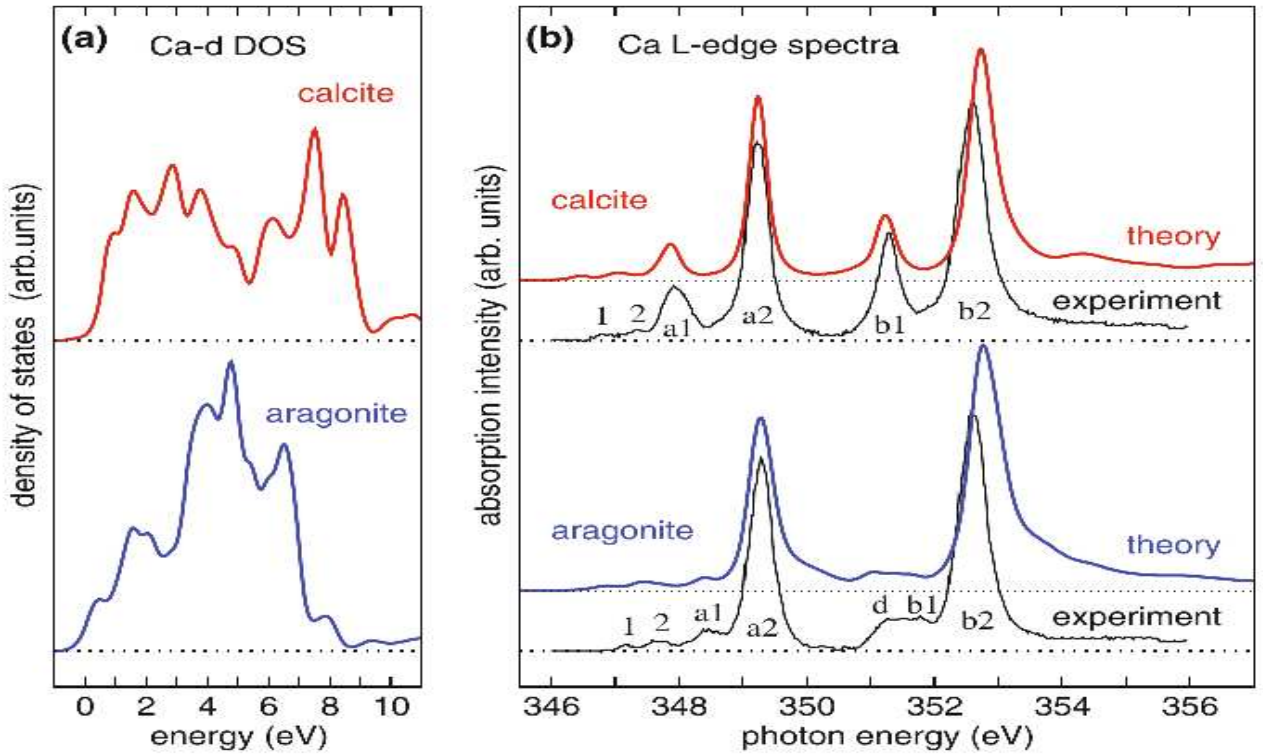

Fig. 12.4 Calcium carbonate ($CaCO_3$) in calcite (*top*) and aragonite phases (*bottom*). **a** Ground state Ca-*d* partial density of states. **b** Ca *L*-edge spectra calculated in multichannel multiple scattering theory [9] along with experimental data taken from [10]

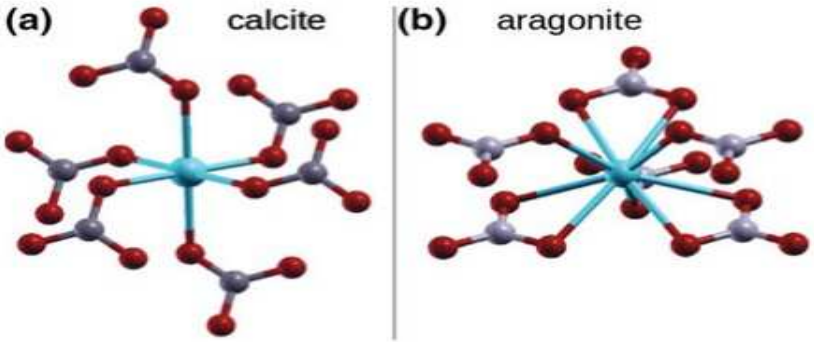

Fig. 12.3 Atomic structure of $CaCO_3$ in **a** calcite and **b** aragonite phases. Ca in *light blue*, C in *dark grey*, O in *red*. One Ca site and its nearest neighbor CO_3 units are shown

XAS: X-ray Absoprtion; complex potential

Alternative form of the GF

$$G(\mathbf{r}_i,\mathbf{r}'_j;E) = \sum_{LL'}\Phi^i_L(\mathbf{r}_i;k)[\boldsymbol{\tau}^{ij}_{LL'}-\delta_{ij}\,T^i_{LL'}]\Phi^j_L(\mathbf{r}_j;k) + \delta_{ij}\sum_{LL'}\Phi^i_L(\mathbf{r}_<;k)T^i_{LL'}\tilde{\Phi}^i_{L'}(\mathbf{r}'_>;k)$$

In this case

$$\sigma_{abs}(\omega)=\sigma_{sct}(\omega)+\sigma_{at}(\omega)$$

where

$$\sigma_{sct}(\omega)=-8\,\pi\,\alpha\,\hbar\,\omega\sum_L \Im M_{L_c\,L}\,(E)\sum_{n=2}^{\infty}[(\mathbf{TG})^n\,\mathbf{T}]^{oo}_{LL}\,M_{L_c\,L}\,(E)$$

$$\sigma_{at}(\omega)=-8\,\pi\,\alpha\,\hbar\,\omega\sum_{LL'}\Im\tilde{M}_{L_c;LL'}\,T^o_{LL'}$$

$$\tilde{M}_{L_c;LL'}=\int_{\Omega_o}\mathrm{d}\mathbf{r}\,\mathrm{d}\mathbf{r}'<\phi^c_{L_c}(\mathbf{r}_o)|\hat{\epsilon}\cdot\mathbf{r}|\Phi^i_L(\mathbf{r}_<;k)\tilde{\Phi}^i_{L'}(\mathbf{r}'_>;k)|\hat{\epsilon}\cdot\mathbf{r}'|\phi^c_{L_c}(\mathbf{r}'_o)>$$

$$\chi(\omega)=\frac{\sigma_{sct}(\omega)}{\sigma_{at}(\omega)}$$

Bouldin et al, Phys. Rev B 38, 10816 (1988)

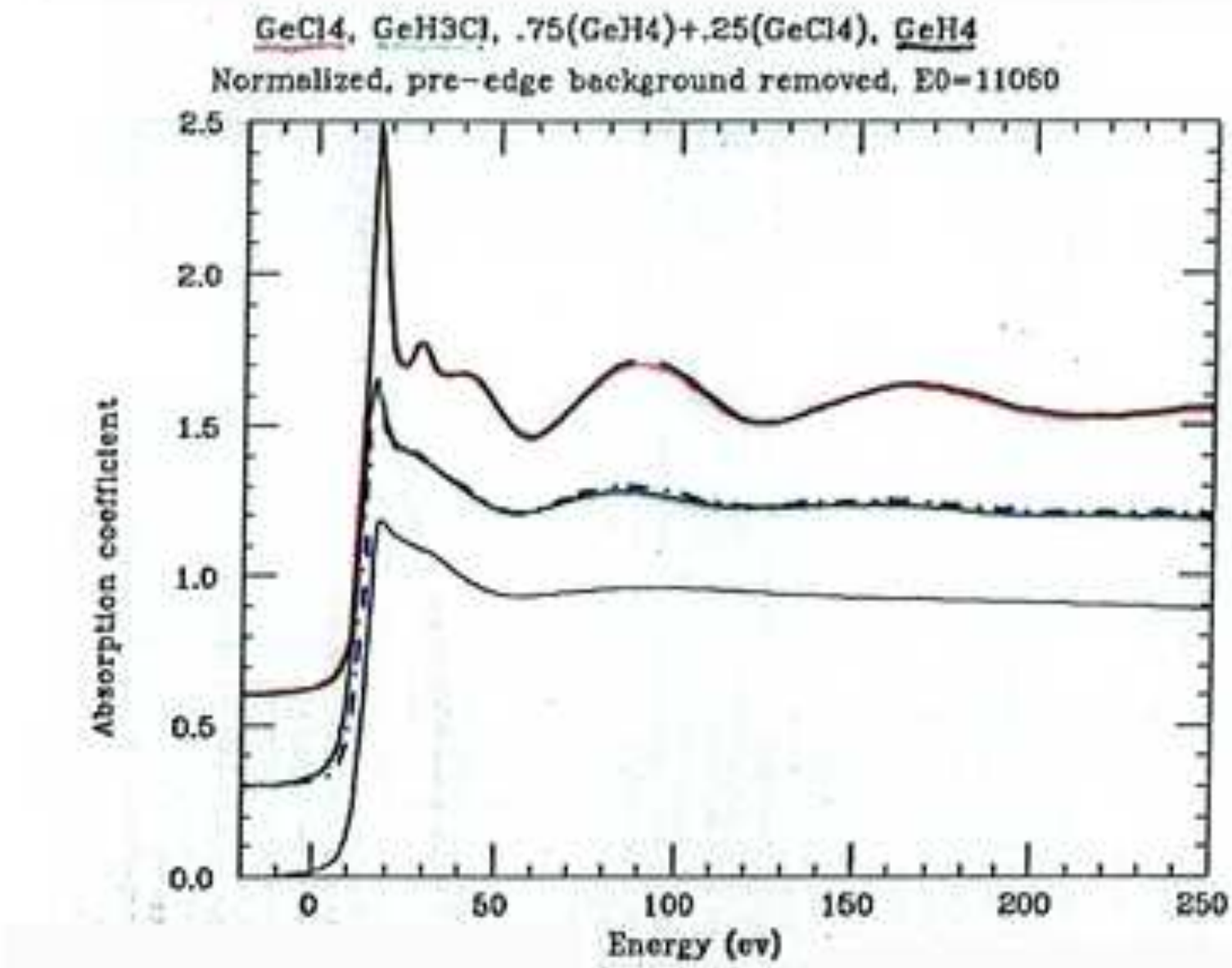

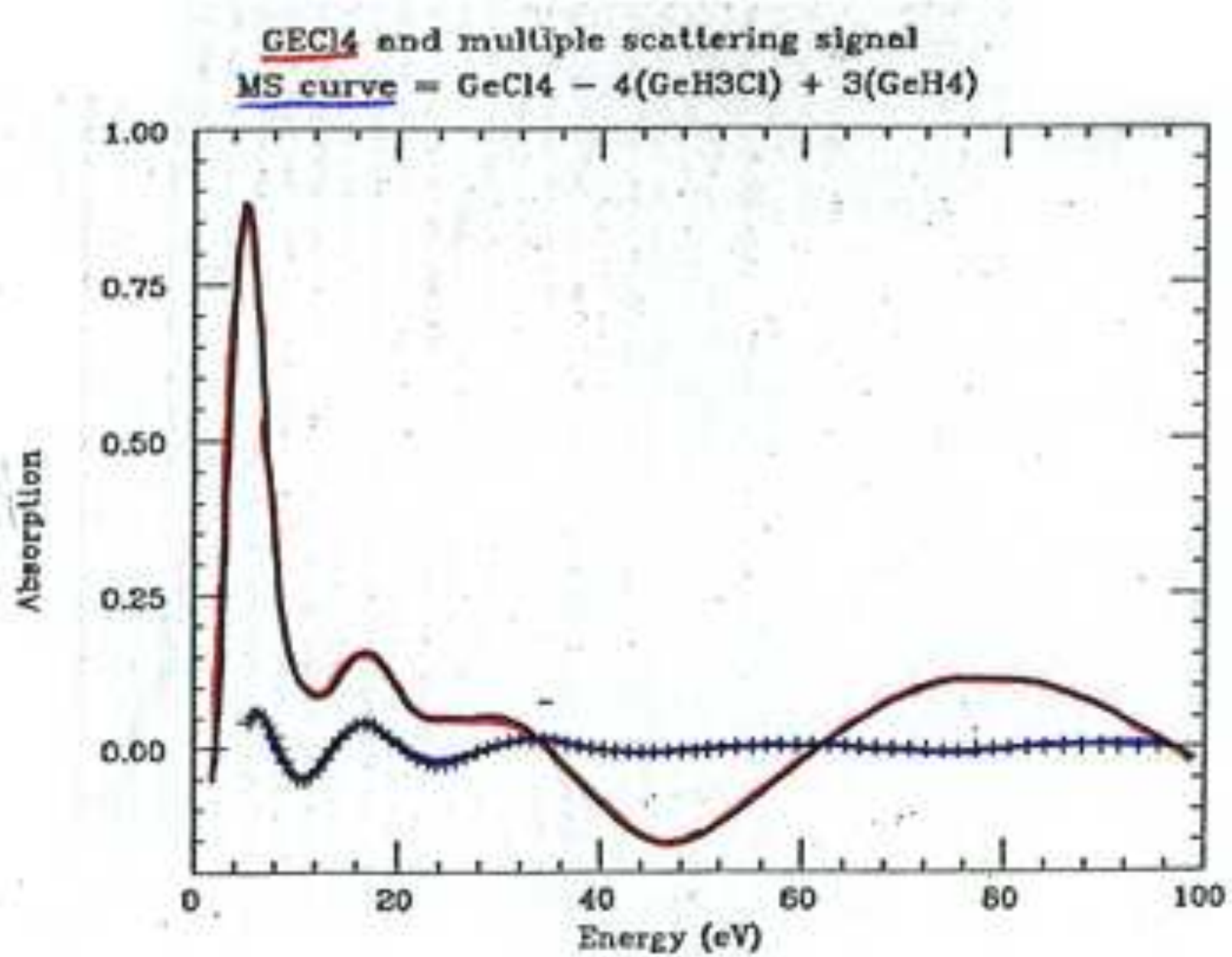
GECl4 and multiple scattering signal
MS curve = GeCl4 − 4(GeH3Cl) + 3(GeH4)
1.00
0.75
0.50
0.25
0.00
Absorption
0
20
40
60
80
100
Energy (eV)

The mean free path: general term of MS series

$$[(\mathbf{TG})^n]^{oo}_{LL'} = \sum_{ij\ldots k} \sum_{L_1 L_2 \ldots L_n} t^o_l \, G^{oi}_{LL_1} \, t^i_{l_1} \, G^{ij}_{L_1 L_2} \, t^j_{l_2} \ldots . G^{ko}_{L_n L'}$$

If $\delta = \delta_1 + i\,\delta_2$

$$kt = \mathrm{e}^{i\delta} \sin\delta = \mathrm{e}^{-2\delta_2}\,\mathrm{e}^{i\delta_1} \sin\delta_1 + \frac{i}{2}\,[1 - \mathrm{e}^{-2\,\delta_2}]$$

$$\Im kt = |kt|^2 + \frac{1}{4}\,[1 - \mathrm{e}^{-4\,\delta_2}] \approx |kt|^2 + \delta_2$$

$$G^{ij}_{LL'} \approx -4\pi\, i^{(l-l')}\, Y_L(\mathbf{R}_i)\, Y_{L'}(\mathbf{R}_j)\, \frac{\mathrm{e}^{i\,k^I R_{ij}}}{k^I R_{ij}}\, g^0_{ll'}(k^I R_{ij})$$

where $k^I = [E - V_I]^{1/2} = k^I_1 + i k^I_2$. For three sites o, i, j the damping is given by an exponential factor with exponent

$$-2\delta^o_2 - k^I_2 R_{oi} - 2\delta^i_2 - k^I_2 R_{ij} - 2\delta^j_2 - k^I_2 R_{jo}$$

In the WKB approximation

$$\delta^j = \int_0^{R_j} [E - V_j(r)]^{1/2} dr - k^I R_j$$

so that, writing $R_{path} = R_{oi} + R_{ij} + R_{jo}$, the damping factor is given by

$$e^{-\kappa_2 R_{path}}$$

where

$$\kappa_2 = \frac{1}{R_{path}} \Im \int_{path} [E - V(r)]^{1/2} dr$$

Therefore

$$\lambda = \frac{1}{2\kappa_2}$$

Usually $[E - V_1(r)] \gg V_2(r)$

$$[E - V(r)]^{1/2} \approx [E - V_1(r)]^{1/2} + \frac{i}{2} \frac{V_2(r)}{[E - V_1(r)]^{1/2}}$$

so that

$$\kappa_2 = \frac{1}{2R_{path}} \int_{path} \frac{V_2(r)}{[E - V_1(r)]^{1/2}} dr \leq \frac{1}{2kR_{path}} \int_{path} V_2(r) dr$$

Finally

$$\lambda(au) = \frac{k(au)^{-1}}{\overline{\Sigma}_2(Ryd)} = \frac{E(Ryd)}{k(au)^{-1}\,\overline{\Sigma}_2(Ryd)}$$

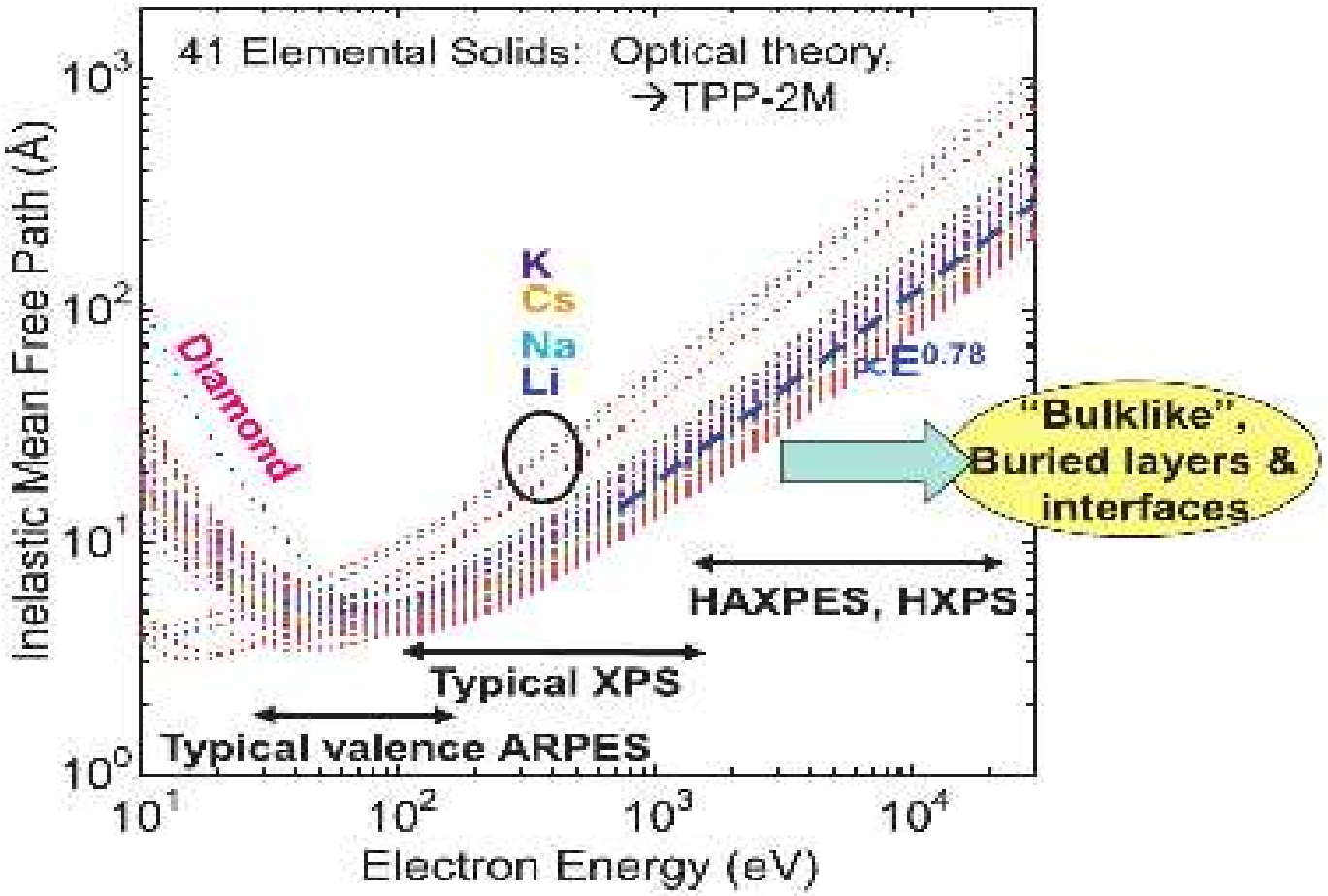

Fig. 2. Energy dependence of electron inelastic mean free paths as calculated from optical properties for 41 elements, with values closely related to the TTP-2 M formula [From ref. 9].

Construction of the Muffin-Tin (MT) potential

Natoli *et al* **J. Synchrotron Rad. 10, 26-42 (2003)**

$$V_c(\mathbf{r}) = -\sum_k \frac{2Z_k}{|\mathbf{r}-\mathbf{R_k}|} + 2\int \mathrm{d}\mathbf{r}' \frac{\rho(\mathbf{r}')}{|\mathbf{r}-\mathbf{r}'|}$$

$\rho(\mathbf{r})$ is obtained by superposition of self-consistent atomic charge densities following Mattheiss prescription

$$\rho^o_{tot}(r) = \rho^o(r) + \sum_j \frac{1}{2R_j r} \int_{|R-r|}^{R+r} \rho_j(r_j) r_j dr_j$$

$$V^o_{tot}(r) = V^o(r) + \sum_j \frac{1}{2R_j r} \int_{|R-r|}^{R+r} V_j(r_j) r_j dr_j$$

$$V_j(r) = 4\pi \left[\frac{2}{r} \int_0^r r_j^2 \rho(r_j) dr_j + 2 \int_r^\infty \rho(r_j) r_j dr_j \right]$$

$$\overline{V}_c = \frac{1}{\Delta\Omega} \int_{\Delta\Omega} V_c(\mathbf{r}) d\mathbf{r} = \frac{1}{4\pi\Delta\Omega} \left[\int_0^{R_o} V_c^o(r) r^2 dr - \sum_j \int_0^{R_j} V_c^j(r_j) r_j^2 dr_j \right]$$

$$\overline{\rho}_{int} = \frac{1}{\Delta\Omega}\int_{\Delta\Omega}\rho(\mathbf{r})d\mathbf{r} = \frac{1}{4\pi\Delta\Omega}\left[\int_0^{R_o}\rho^o_{tot}(r)r^2dr - \sum_j\int_0^{R_j}\rho^j(r_j)r_j^2dr_j\right]$$

Determination of MT radii

Norman radii

$$\int_0^{R_i^{Norm}}\rho^j(r_i)r_i^2dr_i = Z_i$$

Then

$$R_{i(j)} = \frac{R_{i(j)}^{Norm}R_{ij}}{R_i^{Norm} + R_j^{Norm}}$$

Local Density Approximation for $\Sigma(\mathbf{r}; E)$: Hedin-Lundqvist Potential

$$\Sigma(\mathbf{r}; E) \approx \Sigma_h[p(\mathbf{r}), E - V_c(\mathbf{r}); \rho(\mathbf{r})] \equiv V_{exc}(\mathbf{r})$$

Since $E - V_c(\mathbf{r}) \approx p^2(\mathbf{r})$

$$V_{exc}(\mathbf{r}) \simeq \Sigma_h[p(\mathbf{r}), p^2(\mathbf{r}); \rho(\mathbf{r})]$$

$$p^2(\mathbf{r}) + \Sigma_h[p(\mathbf{r}), p^2(\mathbf{r}); \rho(\mathbf{r})] = k^2 + k_F^2(\mathbf{r}) + \Sigma_h[k_F, k_F^2; \rho(\mathbf{r})]$$

$$k_F = (3\pi^2\rho)^{1/3} = \frac{1}{\beta r_s} \qquad r_s = [\frac{3}{4\pi\rho}]^{1/3} \qquad \beta = [\frac{4}{9\pi}]^{1/3} \approx 0.52$$

$$\Sigma_h(p,\omega) = \frac{i}{(2\pi)^4}\int \mathrm{e}^{i\omega'\delta}\frac{V(\mathbf{p}')}{\epsilon(\mathbf{p}',\omega')}G_0(\mathbf{p}+\mathbf{p}',\omega+\omega')d\mathbf{p}'d\omega'$$

$$G_0(\mathbf{p},\omega) = \frac{1}{\omega - p^2 + isign(\omega-\epsilon_F)}$$

$$\frac{1}{\epsilon(\mathbf{p},\omega)} = 1 + \frac{\omega_p^2}{\omega^2 - \omega_1^2(p)}$$

$$\omega_p = 4[\frac{\beta r_s}{3\pi}]^{1/2}\epsilon_F = \frac{41.7}{[r_s(au)]^{3/2}}\,eV$$

$$\omega_1^2(p) = \omega_p^2 + \epsilon_F^2\left[\frac{4p^2}{3k_F^2} + \frac{p^4}{k_F^4}\right]$$

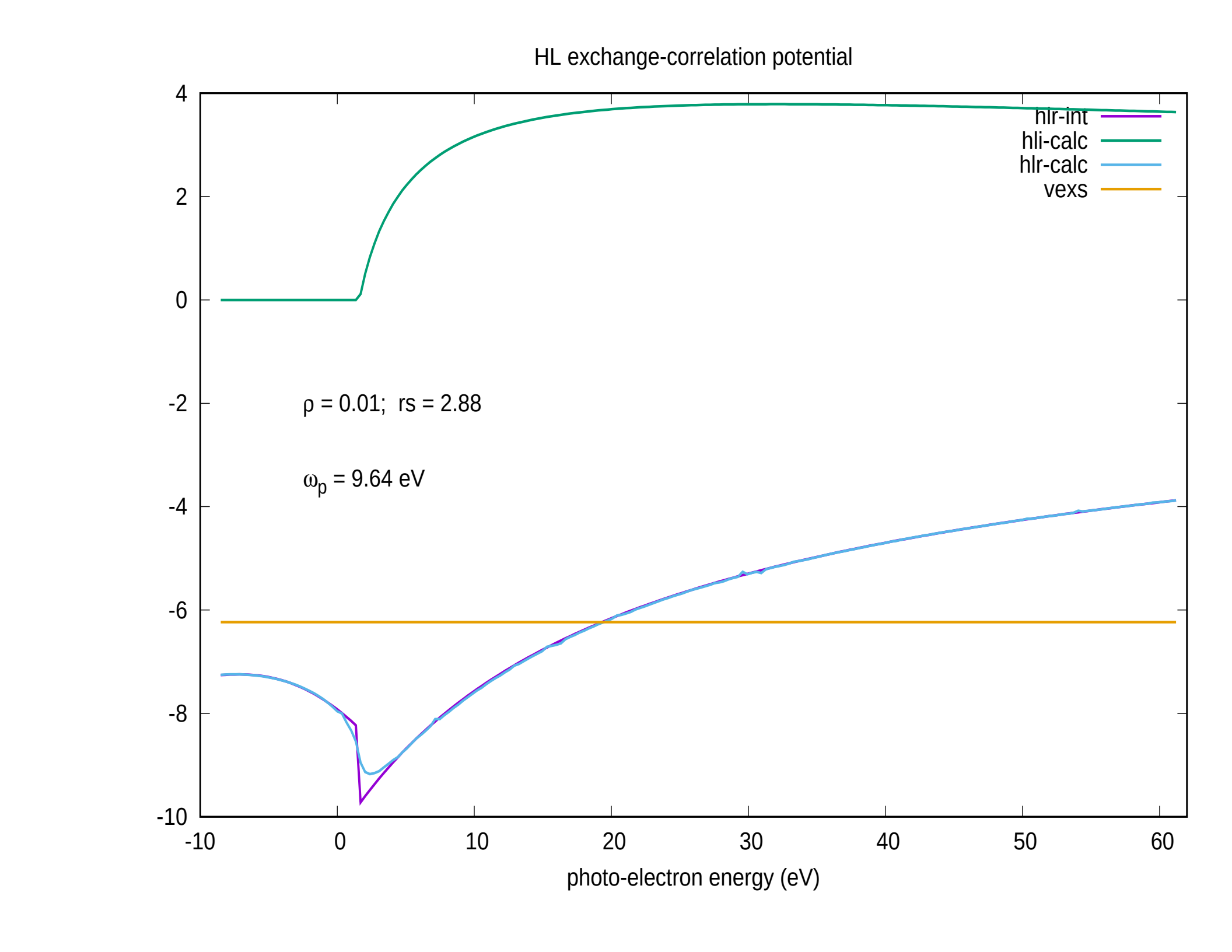
HL exchange-correlation potential
hlr-int
hli-calc
hlr-calc
vexs
ρ = 0.01; rs = 2.88
ω_p = 9.64 eV
4
2
0
-2
-4
-6
-8
-10
-10
0
10
20
30
40
50
60
photo-electron energy (eV)

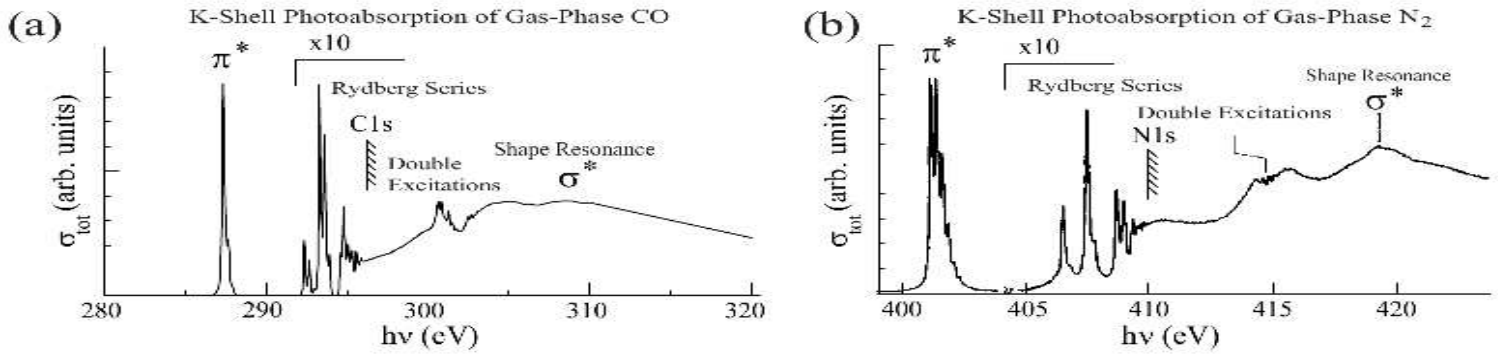

Figure 2.6: High resolution photoabsorption spectrum in the region of **(a)** the carbon K-edge of CO[57] and **(b)** the nitrogen K-edge of N_2.[58]

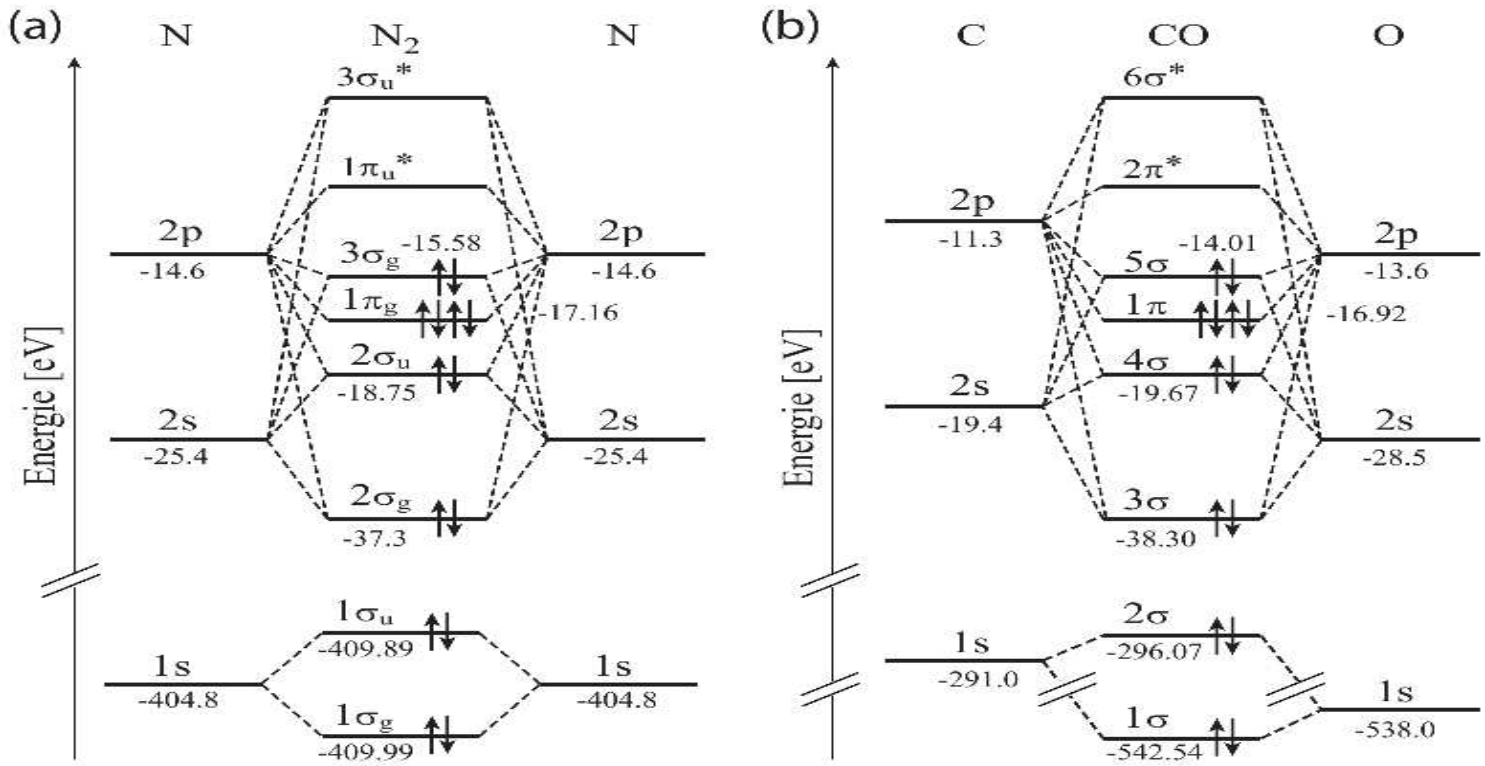

Figure 2.5: Molecular orbitals of the N_2 **(a)** and CO molecule **(b)** in the LCAO model together with their electronic ground state occupation. Molecular binding energies are taken from Hemmers[35] and Hergenhahn ,[44] atomic binding energies are based on calculations by Verner *et al.*[53]

DELOCALIZED INITIAL CORE STATE: THE CASE OF K-EDGE PHOTOABSORPTION OF N_2 MOLECULE

$$\sigma_{tot}(\omega) \propto -\frac{1}{\pi}\Im \int < \phi^c_{L_c}(\mathbf{r}_o)|\hat{\epsilon}\cdot\mathbf{r}|G(\mathbf{r},\mathbf{r}';E)|\hat{\epsilon}\cdot\mathbf{r}'|\phi^c_{L_c}(\mathbf{r}'_o) > \mathrm{d}\mathbf{r}\mathrm{d}\mathbf{r}'$$

What happens if

$$\phi^c_{L_c}(\mathbf{r}_o) \equiv \phi_{g,u}(\mathbf{r}) = \frac{1}{\sqrt{2}}\big(\phi(\mathbf{r}_1) \pm \phi(\mathbf{r}_2)\big)$$

We easily find, remembering the form of the GF:

$$\sigma_{abs}(\omega) = 4\pi\alpha\hbar\omega \left(\sum_{LL'} M_L(E)\Im\boldsymbol{\tau}^{11}_{LL'}M^\star_{L'}(E) \pm \sum_{LL'} M_L(E)\Im\boldsymbol{\tau}^{12}_{LL'}M^\star_{L'}(E) \right)$$

In the Born approximation, from the equation obeyed by the scattering path operator $\boldsymbol{\tau}$

$$\boldsymbol{\tau}^{ij}_{LL'} = T^{i}_{LL'}\delta_{ij} + \sum_{\underline{L}\underline{L}'k} T^{i}_{L\underline{L}}\, G^{i\,k}_{\underline{L}\underline{L}'}\, \boldsymbol{\tau}^{k\,j}_{\underline{L}'L'}$$

$$\boldsymbol{\tau}^{11}_{LL'} \approx t_l \qquad \boldsymbol{\tau}^{12}_{LL'} \approx t_l G^{12}_{LL} t_l$$

Therefore

$$\sigma_{abs} \approx \sigma_{at}\left(1 \pm A_{ll}(kR)\,\frac{\sin(kR + 2\delta_1 + \phi_{ll}(kR))}{kR}\right)$$

This is the generalization of the celebrated COHEN-FANO formula, interpreted as a molecular manifestation of the Young's two slit experiment (H. Cohen and U. Fano, Phys. Rev. **150**, 30 (1966)).

The MS expression however does not support this interpretation.

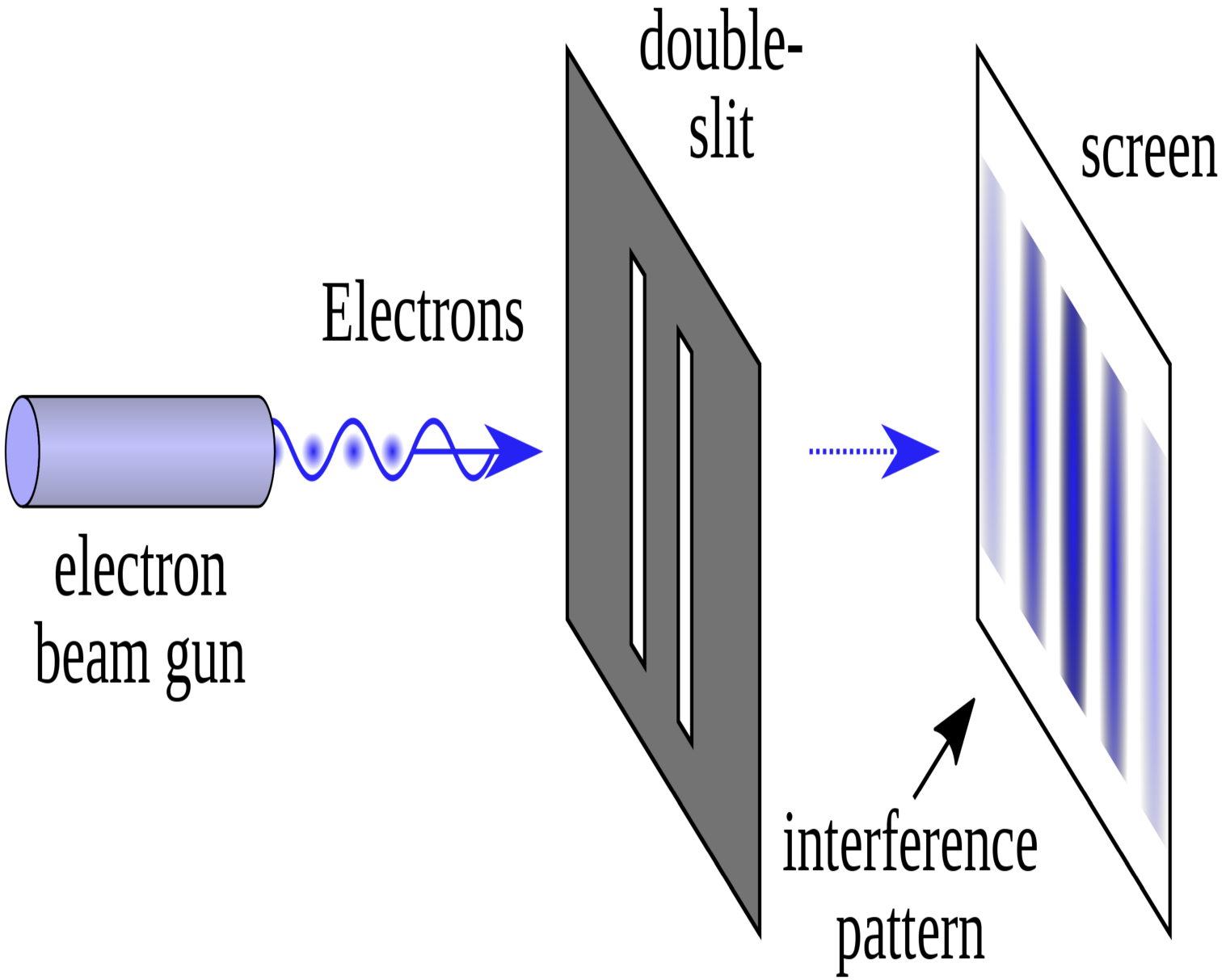
double-
slit
screen
Electrons
electron
beam gun
interference
pattern

U. Becker, Nature.474.586.2011

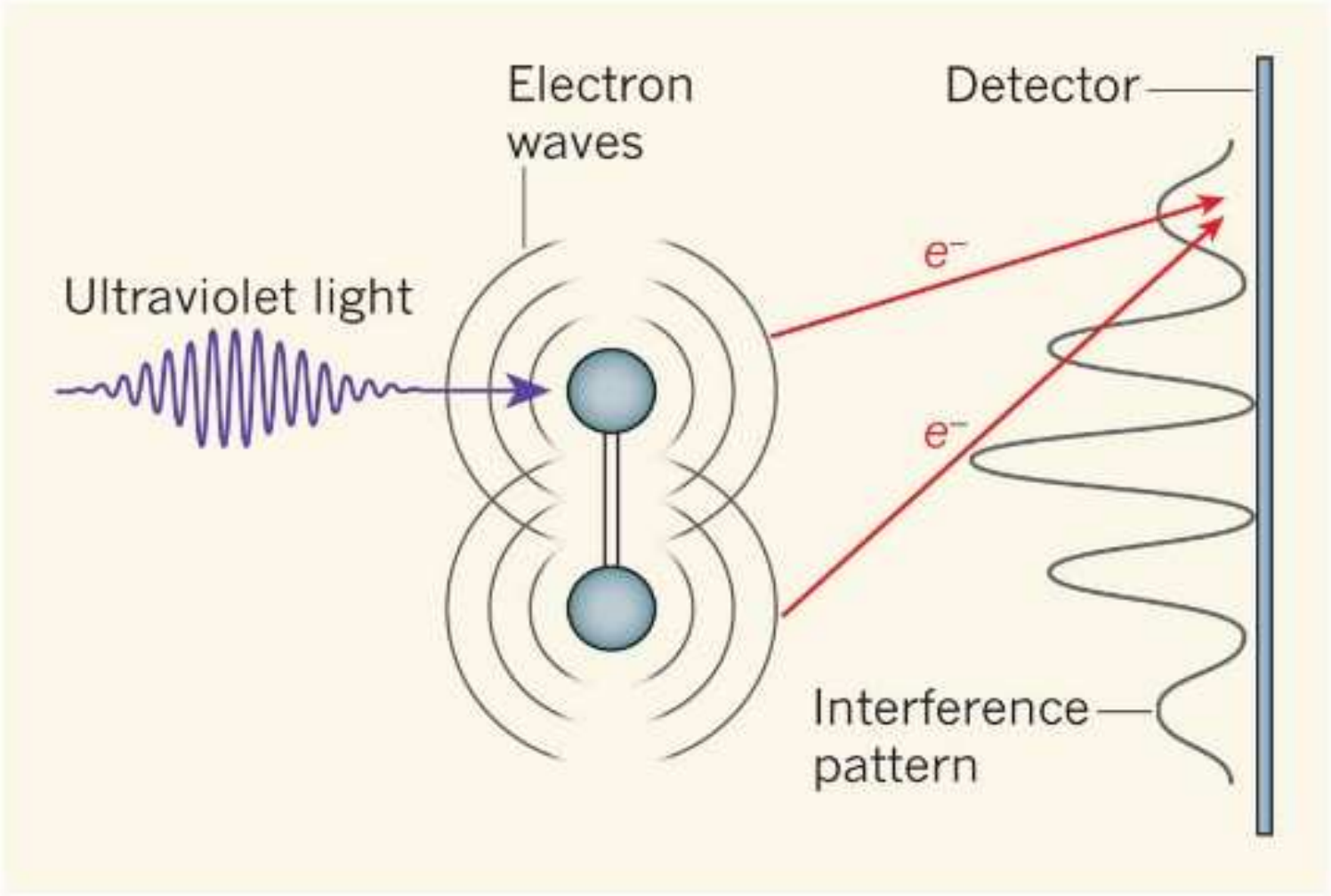

Figure 2.11: The figure is taken from [9] showing the principle of a molecular double slit.

C. R. Natoli, *Synchrotron Radiation Science and Applications; Proceedings of the 2019 Meeting of the Italian Synchrotron Radiation Society - Dedicated to Carlo Lamberti.*
Di Cicco A., Giuli G., Trapananti A., Eds.; Springer Proceedings in Physics, Vol. 220, 17-31 (2021)

THANKS FOR YOUR ATTENTION